UTILIZATION OF REALISTIC PUMPED HYDROELECTRIC STORAGE SYSTEM MODEL FOR VARIOUS OPTIMAL SHORT TERM CONTROL STRATEGIES

A THESIS SUBMITTED TO
THE GRADUATE SCHOOL OF NATURAL AND APPLIED SCIENCES
OF
MIDDLE EAST TECHNICAL UNIVERSITY

BY

OĞUZHAN ÜSTÜNDAĞ

IN PARTIAL FULFILLMENT OF THE REQUIREMENTS
FOR
THE DEGREE OF MASTER OF SCIENCE
IN
ELECTRICAL AND ELECTRONICS ENGINEERING

SEPTEMBER 2019

Approval of the thesis:

UTILIZATION OF REALISTIC PUMPED HYDROELECTRIC STORAGE SYSTEM MODEL FOR VARIOUS OPTIMAL SHORT TERM CONTROL STRATEGIES

submitted by **OĞUZHAN ÜSTÜNDAĞ** in partial fulfillment of the requirements for the degree of **Master of Science in Electrical and Electronics Engineering Department, Middle East Technical University** by,

Prof. Dr. Halil Kalıpçılar
Dean, Graduate School of **Natural and Applied Sciences** _____

Prof. Dr. İlkay Ulusoy
Head of Department, **Electrical and Electronics Engineering** _____

Assoc. Prof. Dr. Murat Göl
Supervisor, **Electrical and Electronics Engineering, METU** _____

Examining Committee Members:

Prof. Dr. Ali Nezih Güven
Electrical and Electronics Engineering, METU _____

Assoc. Prof. Dr. Murat Göl
Electrical and Electronics Engineering, METU _____

Assist. Prof. Dr. Emine Bostancı
Electrical and Electronics Engineering, METU _____

Assist. Prof. Dr. Ozan Keysan
Electrical and Electronics Engineering, METU _____

Prof. Dr. Mehmet Timur Aydemir
Electrical and Electronics Engineering, Gazi University _____

Date:

I hereby declare that all information in this document has been obtained and presented in accordance with academic rules and ethical conduct. I also declare that, as required by these rules and conduct, I have fully cited and referenced all material and results that are not original to this work.

Name, Surname: Oğuzhan Üstündağ

Signature :

ABSTRACT

UTILIZATION OF REALISTIC PUMPED HYDROELECTRIC STORAGE SYSTEM MODEL FOR VARIOUS OPTIMAL SHORT TERM CONTROL STRATEGIES

Üstündağ, Oğuzhan
M.S., Department of Electrical and Electronics Engineering
Supervisor: Assoc. Prof. Dr. Murat Göl

September 2019, 81 pages

Due to ecological problems that we are facing, renewable energy sources, such as wind and solar, are emerging trends. However, unless renewable energy is supported by storage systems, the reliability of supply may decrease because of its intermittent and uncertain nature. Besides, since the generation is not controllable without the storage, profitability in the energy market may be risky. In this context, pumped hydroelectric storage systems are the most common and mature way of store electrical energy in grid level.

In this thesis, Gökçekaya pumped storage power plant, whose feasibility study has been completed by Japan International Cooperation Agency-JICA, has been modeled. The model is discretized to take water level changes into account and piecewise linearized to consider efficiency alterations. Wind generation and market price data are obtained from Energy Exchange Istanbul-EXIST Transparency Platform. Optimization problem is constructed using mixed integer linear programming method with AMPL Language. Problems are solved in NEOS Servers by using CPLEX as a

solver. For the short term, a combination of objective functions, fluctuated generation minimization and profit maximization, have been studied. A small pump unit has been included to the system in order to observe its effects. Operation of each problem has been demonstrated by plotting its results for three consecutive days. Then, one month results are analyzed for January and August. It is found that the small pump unit enhances the operation of the system for all problems. Besides, it is concluded that due to fluctuated electricity market prices, working in January becomes more profitable.

Keywords: Pumped Hydroelectric Storage System, Energy Storage, Mixed Integer Linear Programming

ÖZ

GERÇEKÇİ POMPAJ DEPOLAMALI HİDROELEKTRİK SİSTEM MODELİNİN ÇEŞİTLİ OPTİMAL KISA DÖNEM KONTROL STRATEJİLERİ İÇİN KULLANILMASI

Üstündağ, Oğuzhan
Yüksek Lisans, Elektrik ve Elektronik Mühendisliği Bölümü
Tez Yöneticisi: Doç. Dr. Murat Göl

Eylül 2019 , 81 sayfa

Karşı karşıya kaldığımız ekolojik sorunlardan dolayı rüzgar ve güneş gibi yenilenebilir enerji kaynakları yükselen trend halindedir. Ancak yenilenebilir enerji, depolama sistemleriyle desteklenmediği taktirde, üretimin aralıklı ve belirsiz doğasından dolayı arz güvenirliliği düşebilir. Ayrıca üretim, depolama olmadan kontrol edilebilir olmadığı için enerji piyasasında karlılık riskli olabilir. Bu çerçevede, pompaj depolamalı hidroelektrik sistemler, elektrik enerjisini şebeke seviyesinde depolamanın en yaygın ve olgun yoludur.

Bu tezde, Japonya Uluslararası İşbirliği Ajansı-JICA tarafından fizibilite çalışması tamamlanan Gökçekaya pompaj depolamalı enerji santrali modellenmiştir. Su seviyesindeki değişiklikleri hesaba katmak için model ayrıklaştırılmış, verimlilik değişimlerini göz önüne almak için model parçalı doğrusallaştırılmıştır. Rüzgar üretim ve piyasa fiyat verileri Enerji Piyasaları İşletme Anonim Şirketi-EPİAŞ Şeffaflık Platformundan elde edilmiştir. Optimizasyon problemi, tamsayı karışık doğrusal programlama yöntemi kullanılarak AMPL dili ile oluşturulmuştur. Problemler NEOS sunucu-

larında CPLEX çözücüsü ile çözülmüştür. Kısa dönem için, dalgalı üretimi minimize eden ve karlılığı maksimize eden amaç fonksiyon kombinasyonları çalışılmıştır. Küçük bir pompa ünitesi sisteme dahil edilerek etkileri gözlemlenmiştir. Her bir problemin işleyişi üç günlük sonuçlarının çizilmesiyle gösterilmiştir. Ardından, Ocak ve Ağustos için bir aylık sonuçlar analiz edilmiştir. Küçük pompa ünitesinin tüm problemlerin işleyişini geliştirdiği bulunmuştur. Ayrıca, dalgalı elektrik piyasası fiyatları nedeniyle Ocak ayında çalışmanın daha karlı olduğu sonucuna varılmıştır.

Anahtar Kelimeler: Pompaj Depolamalı Hidroelektrik Sistem, Enerji Depolama, Tamsayı Karışık Doğrusal Programlama

To my family...

ACKNOWLEDGMENTS

First and foremost, I would like to express my sincere gratitude and respects to my supervisor Assoc. Prof. Murat Göl for his advice, guidance, and supports throughout this study.

I am grateful to my managers for their mentorship and help throughout my professional work life. I would moreover thank my dear colleagues for the warm work environment and for being beyond just a colleague.

I would especially like to thank all my friends. It is valuable to me their genuine support in all circumstances.

I could not end this section without conveying my profound gratitude to my family. It would not be possible for me to succeed without their everlasting love and continuous encouragement.

Last but certainly not least, my special thanks go to my wife Büşra Timur Üstündağ for her steadfastness, toleration, support, and trust in me. This work would have never been done without her.

TABLE OF CONTENTS

APPENDICES

LIST OF TABLES

TABLES

LIST OF FIGURES

FIGURES

LIST OF ABBREVIATIONS

ABBREVIATIONS

A	Pipeline Cross-sectional Area [m^2]
API	Application Programming Interface
$c_{1,t}$, $c_{2,t}$	Binary Variables Used for Volume Level Discretization at Time Period t.
D	Inner Diameter of Pipeline [m]
d_t	Binary Status of Turbine at Time Period t.
dif_t	A dummy Variable for Taking Absolute Value.
$\bar{E_d}$, $\underline{E_d}$	Upper and Lower Bounds of Discharged Energy [MWh].
$E_{d,t}$	Discharged Energy at Time Period t [MWh].
$\bar{E_p}$, $\underline{E_p}$	Upper and Lower Bounds of Pumped Energy [MWh].
$E_{p,t}$	Pumped Energy at Time Period t [MWh].
$E_{w,t}$	Sold Wind Energy at Time Period t [MWh].
$E^a_{w,t}$	Actual Wind Energy for Time Period t [MWh].
$E^d_{w,t}$	Deviation in Wind Energy for Time Period t [MWh].
$E^f_{w,t}$	Forecasted Wind Energy for Time Period t [MWh].
EXIST	Energy Exchange İstanbul
f_D	Darcy Friction Factor
g	Gravity of Earth [m/s^2]
H, H_e, H_p	Available Head, Effective Head, Pump Head [m]
H_l	Head Loss Due to Friction [m]
HEPP	Hydro-Electric Power Plant
$\bar{k}_{E_d}$, $\underline{k}_{E_d}$	Upper and Lower Safety Margin Coefficients for Discharged Energy.

$\bar{k}_{E_p}$, $\underline{k}_{E_p}$	Upper and Lower Safety Margin Coefficients for Pumped Energy.
$\bar{k}_{V_u}$, $\underline{k}_{V_u}$	Upper and Lower Safety Margin Coefficients for Upper Reservoir Volume.
L	Pipeline Length $[m]$
mcp_t	Market Clearing Price for Time Period t [$].
MILP	Mixed Integer Linear Programming
P, P_d, P_p	Power, Power Output of Turbine , Power Input of Pump $[W]$
p_t	Binary Status of Pump at Time Period t.
PHES	Pumped Hydro Energy Storage
PHSS	Pumped Hydroelectric Storage System
PSPP	Pumped Storage Power Plant
Q, Q_d, Q_p	Flow Rate, Discharging Flow Rate, Pumping Flow Rate $[m^3/s]$
$\bar{Q_d}$, $\underline{Q_d}$	Upper and Lower Bounds of Discharge Rate $[m^3/s]$.
$Q_{d,t}$	Discharge Rate at Time Period t $[m^3/s]$.
$\bar{Q_p}$, $\underline{Q_p}$	Upper and Lower Bounds of Pump Rate $[m^3/s]$.
$Q_{p,t}$	Pump Rate at Time Period t $[m^3/s]$.
RPC	Remote Procedure Call
T	Time Span for Optimization.
t_f	Final Time Period $[h]$.
t_i	Initial Time Period $[h]$.
V_f	Flow Velocity $[m/s]$
$\bar{V_u}$, $\underline{V_u}$	Upper and Lower Bounds of Upper Reservoir Water Volume $[m^3]$.
$V_{u,i}$	Initial Volume of Upper Reservoir $[m^3]$.
$V_{u,H}$, $V_{u,L}$	Higher and Lower Limits Used for Volume Level Discretization $[m^3]$.
$V_{u,t}$	Upper Reservoir Volume at Time Period t $[m^3]$.

XML	Extensible Markup Language
η, η_d, η_p	Efficiency, Efficiency for Discharging, Efficiency for Pumping [$\%$]
ρ	Density of Water [kg/m^3]

CHAPTER 1

INTRODUCTION

Technological developments and dramatic population growth amplify energy demand all over the world. In 2018, annual energy demand increased by a rate of 2.3% with respect to the year before, which is almost twice as much as the last decade average rate. As a result of fossil fuel dominated energy consumption, CO_2 emissions rose by 1.7% compared to the year before [1]. In order to limit global warming below to 2°C, greenhouse gas emissions should be at least 25% lower than in 2017 by 2030 [2]. In this respect, renewable energy makes a substantial contribution to fulfill this goal. In particular, the European Union aims to reach 32% renewable energy of total energy consumption by 2030, which was 17.4% as of 2017 [3].

While renewable energy generation is increasing rapidly, it brings along challenging problems. Specifically, wind generation, due to its dynamic and uncertain nature, has negative impacts on the grid, including power system stability and reliability [4]. However, thanks to energy storage systems, most of the problems faced can be resolved. Energy storage systems not only improve the grid stability and reliability, but also enhance resilience and flexibility of the network [5].

Energy storage types can be collected under five main categories, which are chemical, electrochemical, electrical, mechanical, and thermal. These main categories and subcategories under them can be seen in Figure 1.1.

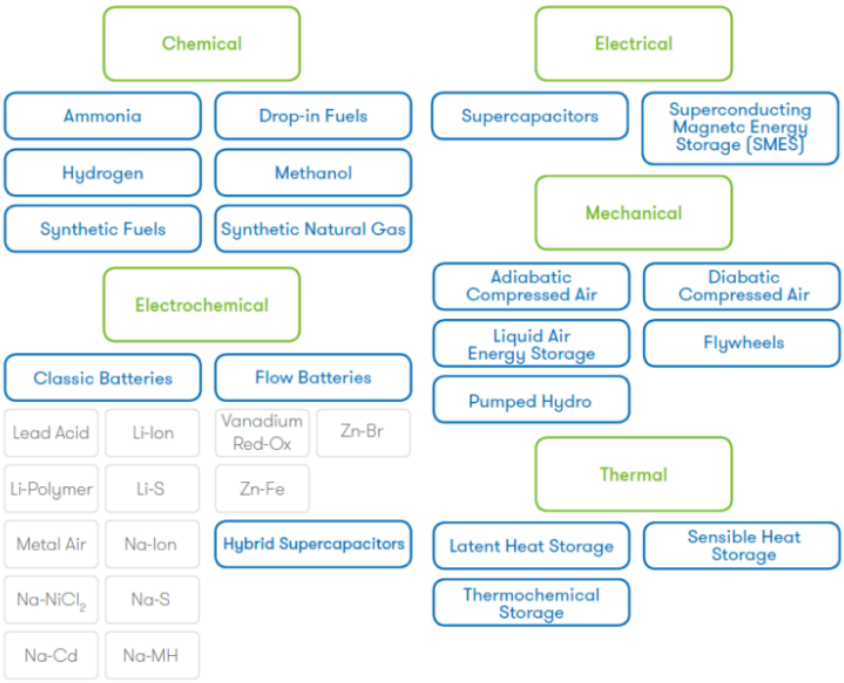

Figure 1.1: Energy Storage Technologies [6]

Among all storage types, pumped hydro storage has the most mature technology [5]. Furthermore, pumped hydro storage dominates the total operational storage capacity with a 98% share, which corresponds to 167.8 GW [7]. Percentages of operational energy storage types are shown in Figure 1.2.

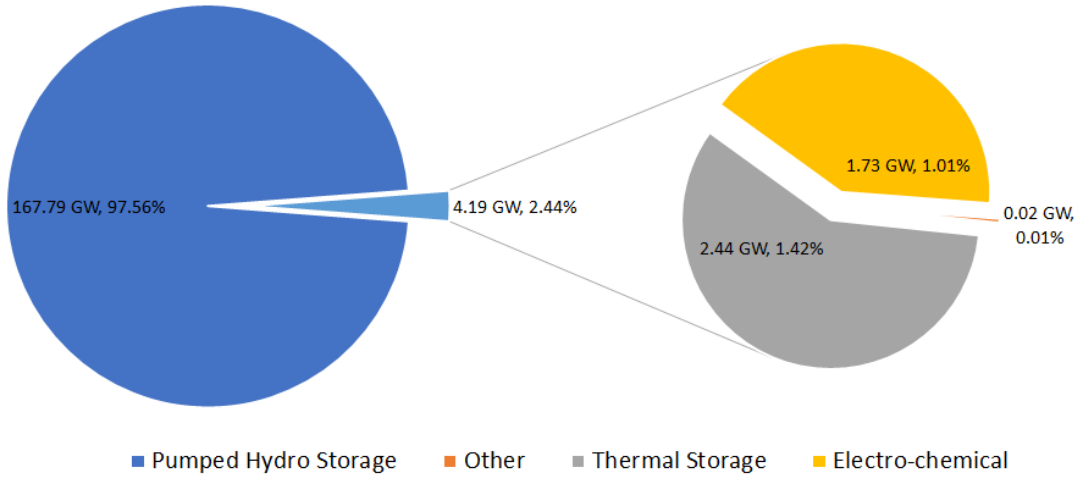

Figure 1.2: Operational Energy Storage Types Share [7]

Historical and projected install capacity of pumped storage systems in the world is given in Figure 1.3a and Figure 1.3b, respectively. It can be noted that installed capacity is increasing determinedly.

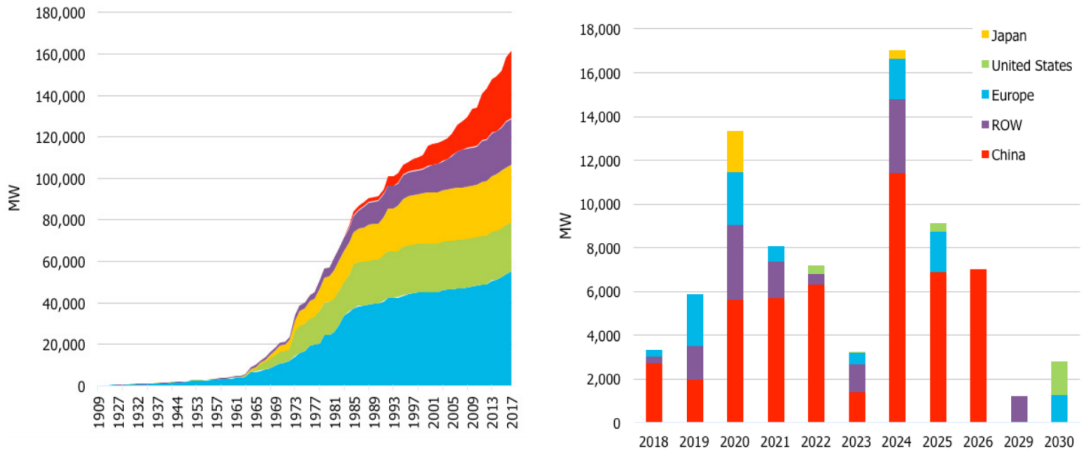

(a) Development of Pumped Storage Installed Capacity

(b) Projected Capacity of Pumped Storage

Figure 1.3: Capacity of the Pumped Storage in the World [8]

Despite not being realistic today, Turkey has a 20 GW wind energy installed capacity target by 2023, which strongly requires the need for energy storage [9]. Although Turkey has the most potential storage capacity for pumped storage in Europe, there is no installed PSPP in Turkey yet [10]. However, a feasibility study was conducted by Japan International Cooperation Agency (JICA) for Turkey [11]. Mainly two projects were considered, Gökçekaya PSPP and Altınkaya PSPP. Motivated by this fact, Gökçekaya PSPP is examined and modelled in this dissertation. On the purpose of acquiring a more realistic model, water level changes in the reservoir is taken into account. Moreover, efficiency changes of the turbine with respect to discharge rate is also considered. Obtained realistic model of Gökçekaya PSPP is utilized in four different short term optimization problems. In addition, coordinated operation between PSPP and wind plants is also studied. This thesis is aimed to show the usage of Gökçekaya PSPP in realistic short term scenarios.

1.1 General Background and Literature Review on Pumped Hydroelectric Storage System

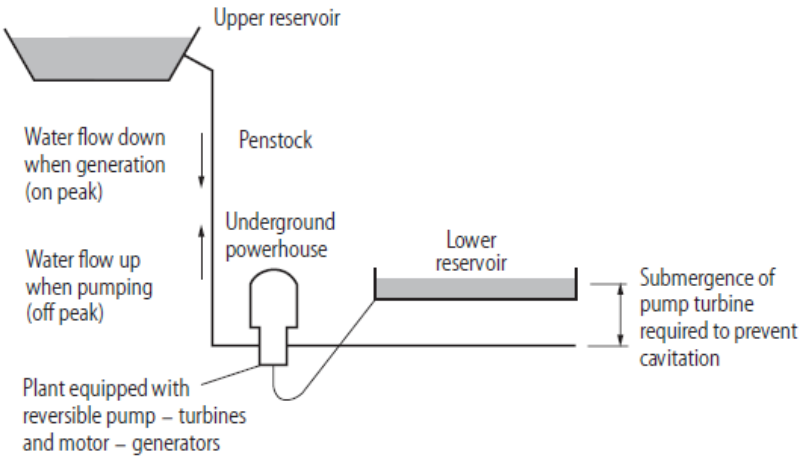

Figure 1.4: Schematic Diagram of a PSPP [12]

Basically, pumped hydroelectric storage system (PHSS) utilizes the potential energy of water by pumping and discharging it between upper and lower reservoirs. When there is low electricity demand in the system, water is pumped to an upper reservoir through a pipeline, at a low price. When there is high demand, implying energy is more valuable, water is discharged to generate electricity. A schematic diagram of pumped storage power plant (PSPP) can be seen in Figure 1.4. PSPP can be classified based on its connection to natural inflow. Closed loop pumped storage reservoirs are not connected to naturally flowing water, while open loop pumped storage has a connection.

Based on its construction, PSPP can be divided into three main parts, which are reservoirs, waterways, and powerhouse. In general, there are two reservoirs located at different heights. The elevation difference between reservoirs is called head, which is an important design criterion for the PSPP. The penstock is the connection between upper reservoir and powerhouse, while the tailrace is the connection between powerhouse and lower reservoir. The powerhouse level is lower than the lower reservoir level to prevent cavitation. This level difference is also known as suction head.

The powerhouse comprises of mechanical components, turbine and pump; electrical components, generator and motor; auxiliary components including transformer, controllers, switching devices.

In terms of power plant configuration, there are three types of setup. A binary setup has one reversible pump-turbine and one motor-generator electrical machine. A ternary setup consists of a separate pump and turbine but single electrical machine as a motor-generator. Last, a quaternary setup has a turbine-generator and pump-motor configuration. Because of financial reasons, binary setup is the most commonly used type [13]. Depending on the head and discharge rate, pump-turbine type may be chosen among Pelton, Francis or Kaplan. In general, due to its wide range of operation, Francis type is commonly used [14, 15].

PHSS has several advantages. Thanks to its fast reaction time, from seconds to a couple of minutes, PSPP can be used in voltage and frequency control. Besides having black start capability, PSPP provides reactive power support as well. Moreover, because the stored energy is only limited to its reservoir sizes, stored energy can reach up to hundreds of GWh [16]. This energy capacity makes pumped storage a crucial part of bulk power management even for a long duration. Furthermore, PSPP can be used for balancing the fluctuated operation of renewable energy sources like wind or solar.

On the other hand, PHSS has some challenges as well. Construction of PSPP has geographical restrictions. That is to say, the environment should be appropriate to construct reservoirs. Also, high initial investment costs and long construction periods decrease the rate of return. While being close to the existing transmission system, PSPP should be respectful to the environment, as well.

Considering all the advantages and the challenges mentioned above, Turkey plans to construct up to 4500 MW of PHSS by 2025 [17]. One of the proposed PSPP for the construction is Gökçekaya, whose main features are shown in Table 1.1. It is planned to have four Francis type reversible pump-turbine units where each is 350 MW, for a 1400 MW total. The PSPP has 428 m^3/s designed discharge and 379.5m effective head which will be explained in the next chapter. A new upper reservoir will be constructed with a 10.8 $mil.m^3$ effective reservoir capacity. For the upper

reservoir, the water level changes from $770m$ to $800m$. The existing Gökçekaya hydroelectric power plant (HEPP) dam is taken as the lower reservoir for the PSPP. It has a 214 $mil.m^3$ effective reservoir capacity and the water level changes from $377.5m$ to $389m$.

Table 1.1: Main Features of Gökçekaya PSPP [11].

Item	Unit	Characteristic	
Unit capacity	MW	350	
Number of units		4	
Installed capacity	MW	1,400	
Designed discharge	m^3/s	428	
Effective head	m	379.5	
Peak duration time	hrs	7	
Type		Francis type pump-turbine	
Upper/Lower Reservoir		Upper	Lower
High Water Level	m	800	389
Low Water Level	m	770	377.5
Effective Reservoir Capacity	$mil.m^3$	10.8	214

Many research groups have conducted several studies on PHSS regarding modeling and utilization. Moreover, traditional hydropower models can be implemented to PHSS as well. Within the scope of this information, various studies are examined in literature to establish a model for Gökçekaya PSPP.

In general, the mixed integer linear programming (MILP) method is mostly used in literature. One of them is conducted by Chang and coworkers. It is reported that the mixed integer linear programming approach is used for short term hydro scheduling in their model. Although efficiency of turbine and minimum-up/minimum down time limits are taken into account, head level is assumed as a constant in the model [18]. Furthermore, Conejo et al. studied self-scheduling of cascaded hydro plants. Binary variables are used to discretize nonlinear, 3-Dimensional production function for three different head levels as unit performance curves. Then, these curves are

piecewise linearized to use in MILP problem. Start-up costs are also modeled [19]. Then, Borghetti et al. enhanced the method in [19] by parameterizing the number of discrete head levels. Moreover, pumping mode is included. However, change in head level is neglected for this mode [20]. Chen et al. also established a MILP based model with head dependency on both pumping and discharging mode for short term generation scheduling [21]. Another study is studied by Tong and coworkers. They analyzed the effects of linearization on solution feasibility. It is underlined that some hydro generation scheduling functions obtained by MILP method may give infeasible results. A MILP based method is presented to guarantee that results stay in a feasible region [22].

Garcia-Gonzalez and Castro studied MILP based short term hydro scheduling. Reservoirs were taken as cascaded and head dependent. The Problem is piecewise linearized by meshing the nonlinear characteristic surface of the hydro unit. It is found that due to the trade off between result accuracy and computational burden, the proposed method might not be suitable for large systems [23]. On the other hand, Hamann and Hug applied piecewise linearization to nonlinear hydropower production function by using triangulation technique and integrated it into a quadratic program. The proposed model was implemented in a model predictive control framework for the sub-hourly optimization of cascade hydropower system [24].

In literature, many research are conducted by taking into account the PSPP and wind generation together. One of these studies is conducted by Castronuovo and Lopes considering the stochastic characteristics of wind. It is shown that wind farm operational profit increases when there is cooperation with pump storage [25]. Alternatively, Bourry et al. focused on minimizing the energy imbalance cost associated with the stochastic nature of wind by using pumped-hydro storage systems. It resulted that strategic coordination between wind farm and storage system decreases energy imbalance penalty risk [26]. Duque et al. worked on a method which has two simultaneous objectives. The method aims to maximize daily revenue, while it offers a capacity to balance wind forecast errors. In order to determine the size of reserve capacity, a statistical method which estimates the wind power uncertainty is developed [27]. Varkani et al. modelled the integrated operation of wind and pumped storage plants both in energy, spinning and regulation reserve markets by using mixed inte-

ger nonlinear programming technique [28]. Castronuovo et al. studied an integrated approach for cooperation of wind farms and pumped storage plant. They presented three methods with different aims including larger profit and lower imbalance cost. It is found that higher revenue can be obtained with optimal operation [29].

It can be concluded that while some of the studies focused on detailed modelling of the hydro units, others focused on utilizing the pumped hydro storage with renewable generation but using a constant head/efficiency PSPP model. In this dissertation, PSPP model, which considers both head level and efficiency changes, is utilized with wind energy participation. Moreover, short term scheduling for Gökçekaya PSPP model is investigated for various objectives.

1.2 Turkish Electricity Market Structure

Deregulation of the energy sector in the last decades affected the market structure in Turkey. With the aim of being reliable, transparent, nondiscriminatory, and competitive, the current structure of Turkish electricity market can be seen in Figure 1.5.

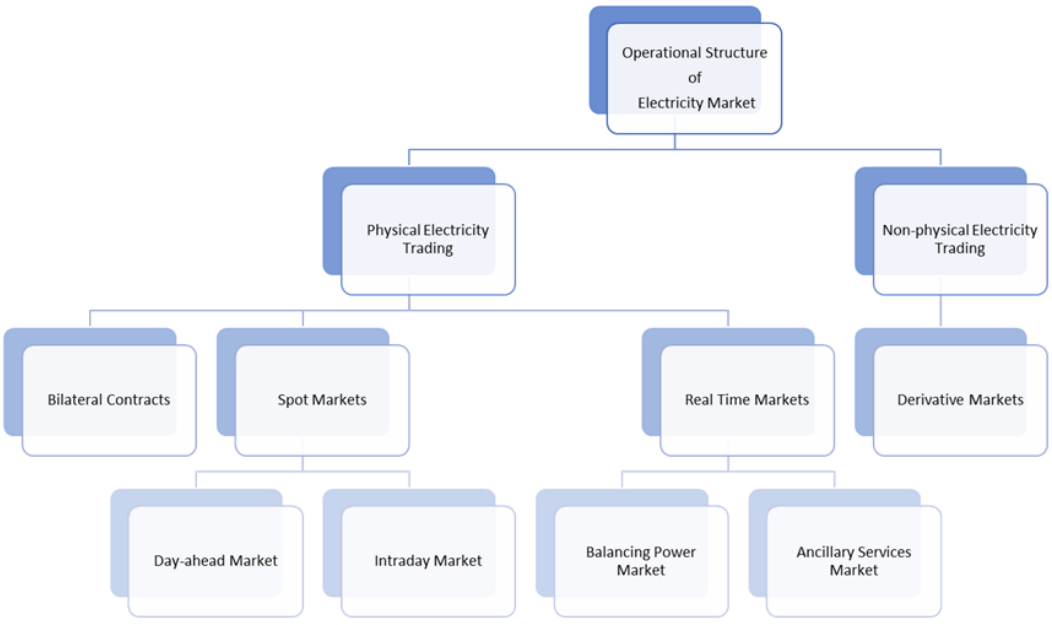

Figure 1.5: Electricity Market Structure in Turkey [30].

1.2.1 Spot Market

Spot market, which is used for electricity trading and balancing, is operated by the independent market operator Energy Exchange İstanbul, EXIST, in Turkey. These actions are conducted in two main markets regarding timing. These markets are day-ahead and intraday markets.

1.2.1.1 Day-ahead Market

Day-ahead market is the mechanism where market participants, energy buyers and energy sellers, can actively participate to trade energy. Nevertheless, it is not mandatory to trade in Day-ahead market. The market is conducted daily on an hourly basis. Each Day (D), which consists of 24-hour time slots, starts at 00:00 and ends when the next day starts, i.e., 00:00 (D+1). Market participants can submit buying and selling bids to the market from 5 days before (D-5) to 1 day before (D-1). Indeed, the deadline to submit a bid is at 12:30 (D-1) [31]. Until 13:30 (D-1), the optimization problem, which aims for maximum daily market surplus, is solved while keeping the balance between supply and demand at each hour [32]. As a result of the problem, market clearing prices and matched volumes are determined and announced for each hour of the day (D).

1.2.1.2 Intraday Market

Intraday market enables market participants to trade 1 hour before the physical delivery. Besides increasing market liquidity, it helps to minimize energy imbalances. The trading method of the market is continuous bilateral trading [33]. Orders should be matched based on time and price. The highest buying and the lowest selling price have priority. When the orders' prices are the same, earlier offers are at the forefront [34].

1.2.2 Real Time Market

Real time market, which comprises power balancing market and ancillary services market, is operated by the Turkish Electricity Transmission Corporation, TEİAŞ, in Turkey. This market improves system security and reliability in real time.

1.2.2.1 Power Balancing Market

Although day-ahead and intraday market helps to minimize power imbalances, there could be unforeseen events that disrupt the balance such as outages or power surpluses. This market ensures that operation frequency deviates from system frequency, 50 Hz, as little as possible. Power plants which can increase or decrease their production by at least 10 MW within 15 minutes are called balancing units. Balancing units are the market participants and they should participate to the market. Balancing units should submit loading and deloading bids to the market. TEİAŞ evaluates the bids and calculates the system marginal price based on system direction and net volume.

1.2.2.2 Ancillary Services Market

Ancillary services market consists of primary and secondary frequency control and supply of reactive power support. Active output of the generator automatically changes in primary frequency control system. In secondary frequency control, active output is set to a value by the central system. Lastly, reactive power support helps to balance reactive power in case it is needed.

Figure 1.6 shows the timeline of Turkish electricity market. Flow starts from bilateral contracts and financial markets. Then continues with day-ahead and intraday markets. Finally, real time markets are the last part of the chain.

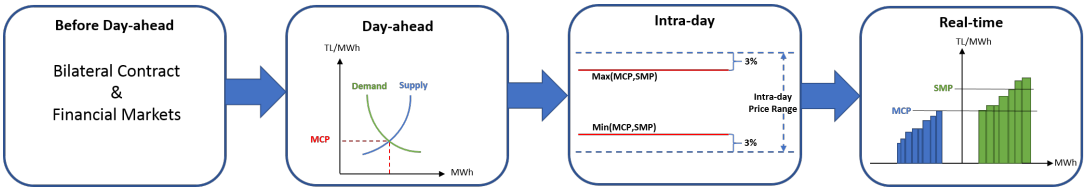

Figure 1.6: Timeline of Turkish Electricity Market [35]

Figure 1.7 shows the market share based on their types for 2018. It can be seen that bilateral contracts still have the majority of the operations in the market.

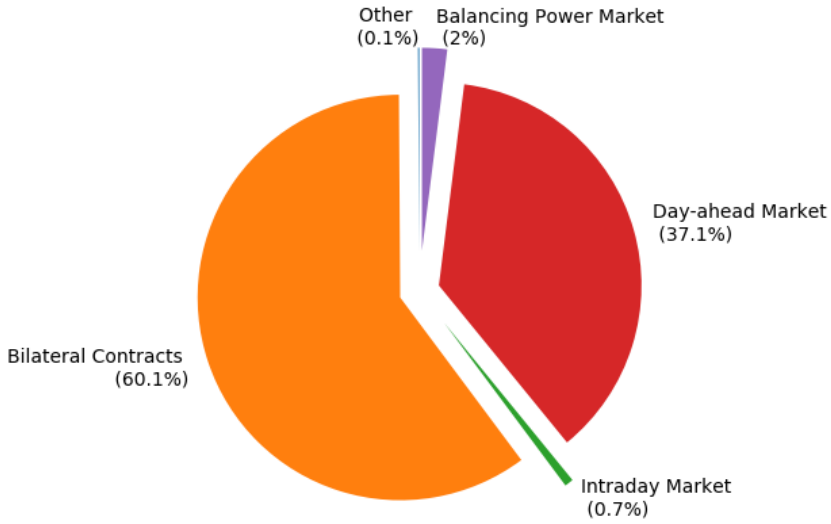

Figure 1.7: Volume Share of Electricity Market in 2018 [36]

To conclude, market participants may have different strategies in this structure, depending on their generation/consumption characteristics and objectives. In this dissertation, a PSPP and wind plants system is desined to participate in day-ahead market to make a profit. On the other hand, PSPP may also participates in balancing power market to compensate energy imbalances due to wind forecast errors.

1.3 Thesis Outline

This dissertation composes of five chapters following the introduction. In Chapter 2, all formulations related with both discharging and pumping modes of PSPP are explained. In light of this information, models for Gökçekaya Pump Storage Power Plant are proposed in detail. Then, Chapter 3 focus on realization of these models in order to perform short-term scheduling optimization for different objectives. Implementations of each aim are clearly stated by introducing objective functions, constraint equations and algorithms. Wind energy modelling utilized in optimization problems are also described in the chapter. Scheduling results of each problem are presented in Chapter 4. The detailed comparison between the results of the problems are declared in the same chapter. Finally, in the last chapter, the results of the dissertation are summarized as a conclusion.

CHAPTER 2

REALISTIC MODELLING OF THE PSPP

In this chapter, pumped hydroelectric storage system of Gökçekaya is modelled for discharging and pumping modes. In these models, it is aimed to simulate more realistic operation of the system without compromising simulation speed. For this purpose, originally non-linear systems are reduced to piecewise linear models.

2.1 Theoretical Background

In an ideal case, the power output of a hydro turbine module or the power input of a hydro pump module, $P\ (W)$, can be calculated by using a formula in Equation (2.1).

$$P = g\rho HQ \tag{2.1}$$

where $H\ (m)$ is available head, which is the elevation difference between the tops of the upper and the lower reservoirs, and $Q\ (m^3/s)$ is the flow rate of water in pipeline. g, gravity of the Earth, and ρ, density of water, are constants and taken as 9.81 m/s^2 and 1000 kg/m^3, respectively.

When a non-ideal case is considered, efficiency should be taken into account. For the turbine module, the overall efficiency factor of discharging, η_d, is multiplied by Equation (2.1). A formula regarding this case can be found in Equation (2.2).

$$P_d = \eta_d g\rho H_e Q_d \tag{2.2}$$

where $P_d\ (W)$ is the power output of turbine, $H_e\ (m)$ is the effective head and

Q_d (m^3/s) is the discharging flow rate.

The efficiency factor of discharging in the formula is the multiplication of turbine efficiency, $\eta_{turbine}$, generator efficiency, $\eta_{generator}$, and transformer efficiency, $\eta_{transformer}$, as seen in Equation (2.3).

$$\eta_d = \eta_{turbine}\eta_{generator}\eta_{transformer} \tag{2.3}$$

Moreover, the available head in Equation (2.1) is replaced by H_e, which is obtained by subtracting the head loss, H_l, from the available head. The relation is given in Equation (2.4).

$$H_e = H - H_l \tag{2.4}$$

Head loss represents dissipated energy due to friction in the pipeline. It is calculated by using a formula known as Darcy-Weisbach Equation which is given in Equation (2.5) [37].

$$H_l = f_D\left(\frac{L}{D}\right)\left(\frac{V_f^2}{2g}\right) \tag{2.5}$$

where f_D is the Darcy Friction Factor, L (m) is pipeline length, D (m) is the inner diameter of pipeline, and V_f (m/s) is flow velocity. V_f can be found by using formula in Equation (2.6).

$$V_f = \frac{Q}{A} \tag{2.6}$$

where A (m^2) is pipeline cross-sectional area, whose formula is given in Equation (2.7).

$$A = \frac{\pi D^2}{4} \tag{2.7}$$

When Equation (2.6) and (2.7) are substituted into Equation (2.5), Equation (2.8) can be obtained.

$$H_l = 8 f_D \left(\frac{L}{D^5} \right) \left(\frac{Q^2}{\pi^2 g} \right) \tag{2.8}$$

It is clear that H_l is directly proportional with L. Furthermore, head loss is inversely proportional and firmly dependent to D. It implies that the horizontal distance between two reservoirs should be small and the inner diameter of pipeline should be large for less head loss. f_D, which is another parameter in the equation can be found by using the Moody Diagram [38]. An illustration of Moody Diagram is shown in Figure A.1 [39].

On the other hand, for pump module, input power can be calculated by using Equation (2.9).

$$P_p = \frac{g \rho H_p Q_p}{\eta_p} \tag{2.9}$$

where P_p (W) is power input of the pump, H_p (m) is pump head, Q_p (m^3/s) is pumping flow rate, and η_p is overall efficiency factor of pumping.

It is obvious that Equation (2.1) is divided by η_p, in contrast to the turbine module. Similar to the efficiency factor of discharging, pumping efficiency factor is the multiplication of three efficiencies, which are pump efficiency, η_{pump}, motor efficiency, η_{motor}, and transformer efficiency, $\eta_{transformer}$, which can be seen in Equation (2.10).

$$\eta_p = \eta_{pump} \eta_{motor} \eta_{transformer} \tag{2.10}$$

Moreover, different than the discharging case, head loss is added to available head to find the pump head in this case as shown in Equation (2.11).

$$H_p = H + H_l \tag{2.11}$$

Energy flow of PSPP is shown in Figure 2.1. It is shown as a Sankey diagram where

all individual components of efficiency are illustrated. First, electrical energy is given to the PSPP as an input. Then, after losses, 86.4% of it can be stored as potential energy in a pumped storage system. Finally, 77.3% of input energy can be recovered as electrical energy. These are typical values for the PSPP [12]. As can be also seen in the figure, the least efficient components of the PSPP are the pump and turbine. Moreover, efficiency of the turbine can decrease down to 70% depending on the discharge rate and the head level [40]. For this reason, more accurate results can be obtained if the turbine efficiency is considered. Thus, the model in this dissertation takes variable turbine efficiency into account besides the other constant efficiencies.

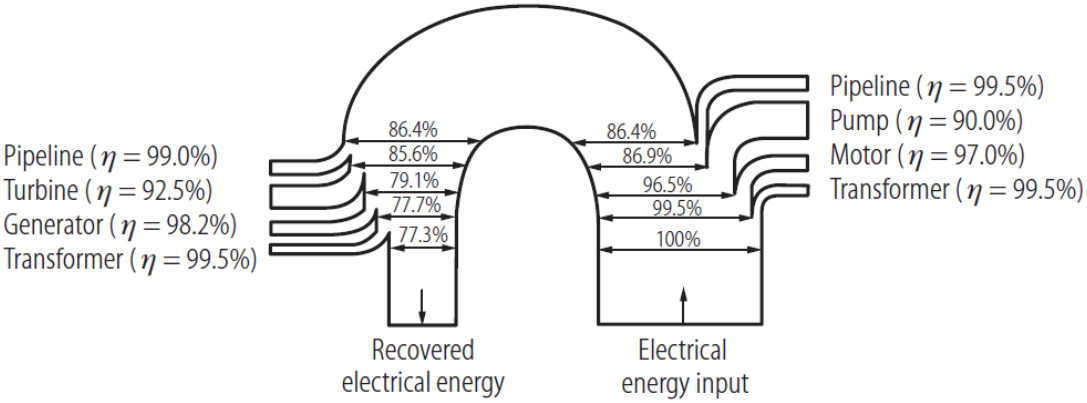

Figure 2.1: Sankey diagram of typical PSPP efficiencies [12].

2.2 Gökçekaya Pumped Storage Power Plant Model

The Gökçekaya PSPP model comprises of discharging and pumping models. Required technical specifications of Gökçekaya PSPP are obtained from JICA reports [11, 41].

2.2.1 Discharging Model

The efficiency of a turbine is a nonlinear function of the discharge rate, Q_d, and effective head, H_e. The function can be calculated using either an experimental setup or using simulation software. The calculated efficiency function is drawn as performance curves to Hill chart. Unfortunately, Hill chart for Gökçekaya PSPP is not available in

the report. Since Kadıncık 2 HEPP has the same turbine type as Gökçekaya PSPP, the Hill chart for Kadıncık 2 HEPP is used as a basis in this dissertation [42]. Kadıncık 2 HEPP Hill chart is scaled to the ranges of Gökçekaya PSPP by using characteristic values which are effective head, discharge rate, power output and turbine efficiency. These are given for maximum, normal and minimum head values in Table 2.1.

Table 2.1: Main Characteristics of Gökçekaya PSPP [11].

Turbine/Pump		Turbine	Pump
Effective head/Pump head	m		
Maximum		396.6	439.7
Normal		379.5	-
Minimum		353.2	398.5
Discharge	m^3/s		
at maximum head		100.3	71.2
at normal head		107.0	-
at minimum head		103.8	82.0
Output/Axial input	MW		
at maximum head		357.5	336.7
at normal head		357.5	-
at minimum head		320.4	353.9
Efficiency	%		
at maximum head		91.7	91.1
at normal head		89.9	-
at minimum head		89.2	90.5
Generator/Motor efficiency	%	97.9	98.3
Total efficiency	%	88.0	89.0

Modified Hill chart can be found in Figure B.1. It is noteworthy that head loss is not calculated since effective head and pump head is already given in the report [11].

By using the modified Hill chart and plot of turbine model for Gökçekaya PSPP in Figure B.2, a nonlinear discharging model for Göçekaya PSPP is created. Moreover,

generator and total efficiency given in Table 2.1 is also added to the model. This nonlinear model is a function of effective head and discharge rate which is shown in Figure 2.2.

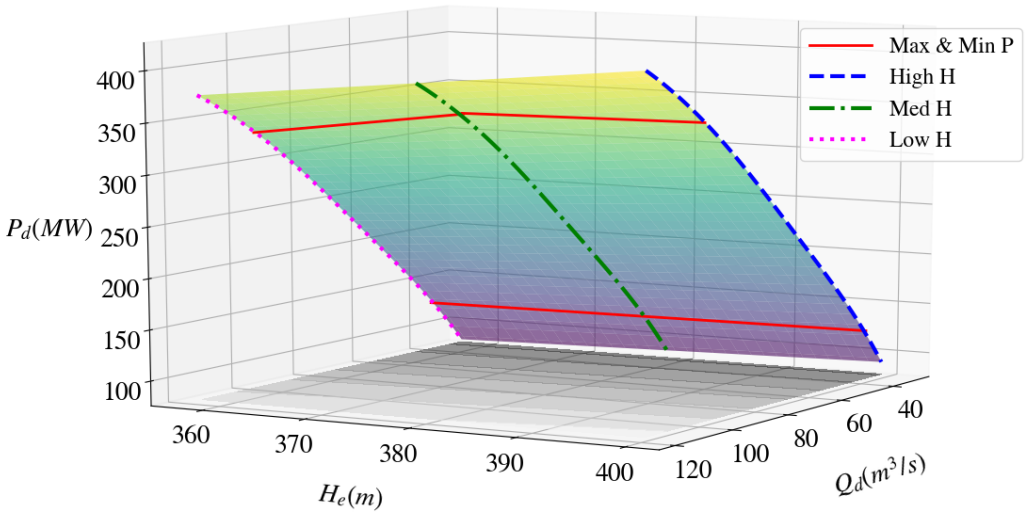

Figure 2.2: Gökçekaya Nonlinear Discharging Model.

It is obvious that power output of the turbine is strongly dependent to discharge rate. On the other hand, change in effective head slightly affects the power output. For this reason, head level is discretized as maximum (high), normal (medium) and minimum (low) head level. Then, by using the discrete efficiency values from the modified Hill chart, piecewise operation curves are obtained for those three head levels. High, medium, and low head level curves have 12, 16, and 15 pieces, respectively. After, by using the Ramer-Douglas-Peucker algorithm [43, 44], the number of pieces for three different head level is reduced to 4 pieces for each head level, to reduce the computational burden. The discharging model, which is discretized by head levels and obtained/reduced piecewise linearized, can be found in Figure 2.3.

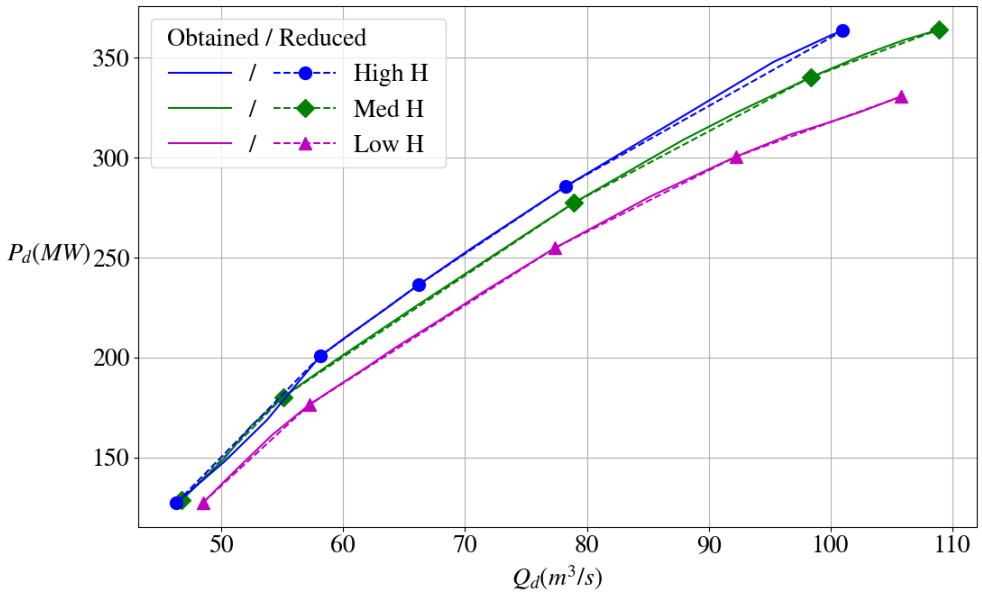

Figure 2.3: Gökçekaya Discretized and Piecewise Linearized Discharging Model.

Figure 2.4 shows the area between obtained and reduced lines with respect to the number of pieces. It can be seen that after four pieces, the area is getting much smaller. For this reason, obtained lines are reduced to four pieces.

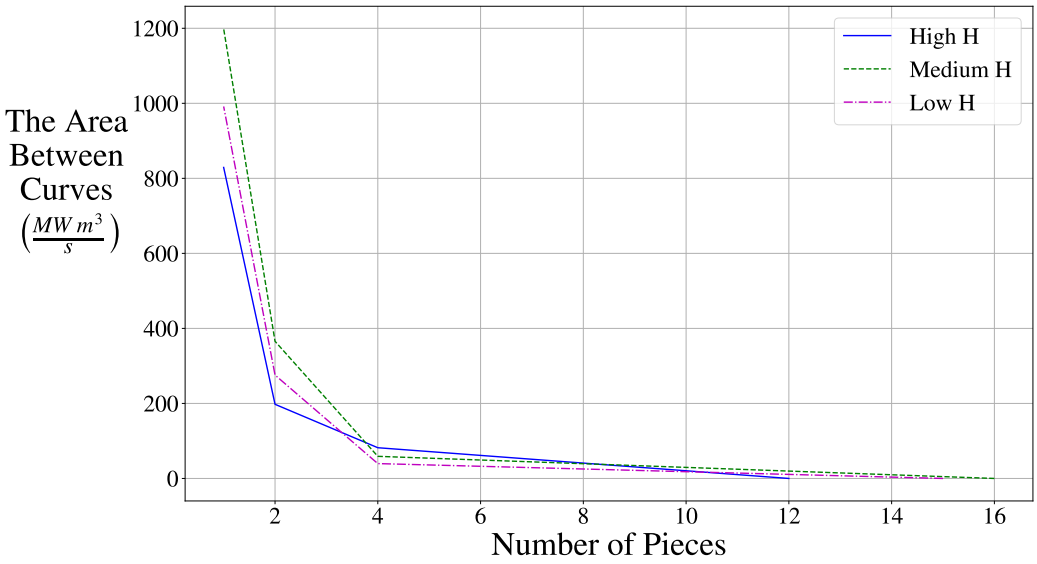

Figure 2.4: Analysis for Number of Piece.

2.2.2 Pumping Model

Since pump efficiency is less affected by change in head levels when compared with turbine efficiency, which can be seen in Table 2.1, efficiency of the pump is taken as a constant in the model. Besides the motor and total efficiency in the table, the plot of pump model for Gökçekaya PSPP in Figure B.3 is used to attain a nonlinear pumping model as shown in Figure 2.5.

Analogous to the discharging model, pumping power, which is the input power, is strongly coupled with the pumping discharge rate. Thus, this nonlinear pumping model is discretized for three different head levels as well. For each head level, input power versus pump flow rate can be plotted as in Figure 2.6.

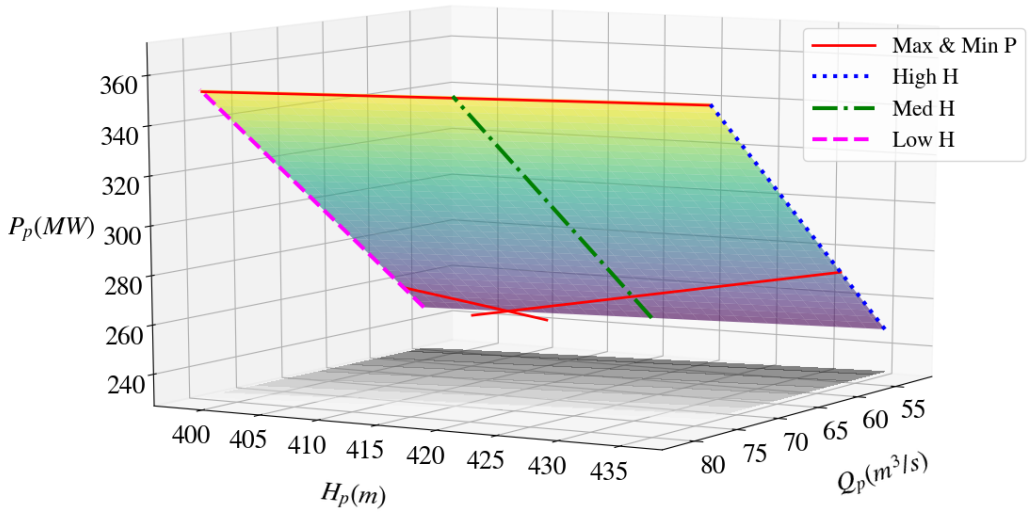

Figure 2.5: Gökçekaya Nonlinear Pumping Model.

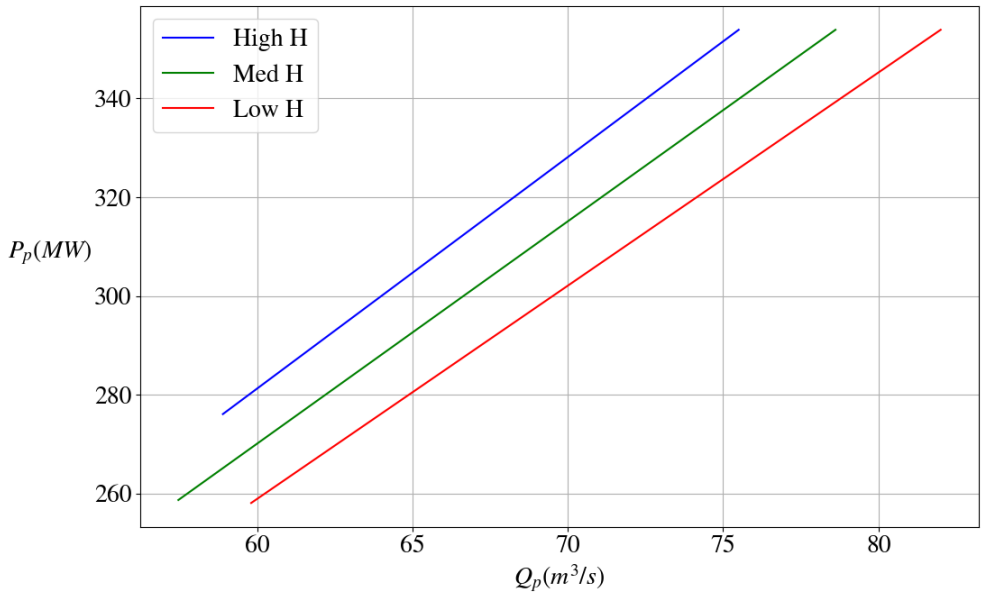

Figure 2.6: Gökçekaya Discretized and Linearized Pumping Model.

2.3 Conclusion

In this chapter, PSPP is modelled, in particular for Gökçekaya PSPP. In order to obtain a more realistic model, change in head is considered for both discharging and pumping mode instead of using a single fixed head value. For that purpose, model is discretized for three different head levels. Moreover, efficiency of the turbine is taken as a function of head and discharging rate for the discharging mode. After that, for each discrete head level, reduced piecewise linearized model is obtained.

CHAPTER 3

OPTIMAL CONTROL FOR DIFFERENT OBJECTIVES

In this chapter, the model described in Chapter 2 is utilized for the frequently addressed problems in literature, mainly profit maximization or imbalance minimization. A combination of these is discussed under four different problem scenarios. First, in Problem I, PSPP acts as a market participant in the day-ahead market and aims for maximum profit. Second, in Problem II, the same objective is desired in the market, but cooperation with wind power plants in the same hypothetical portfolio. In this problem, forecasted wind energy is utilized and actual wind generation is not considered. Third, in Problem III, the purpose of the PSPP is minimizing power imbalances due to wind forecasts in the balancing power market. For this purpose, both actual and forecasted wind energy are included to the problem. Fourth, in Problem IV, while PSPP and wind power plants cooperate in the day-ahead market to maximize profit, PSPP aims to compensate wind energy imbalances in the balancing power market. Similar to Problem III, actual and forecasted wind energy data are utilized in the problem.

Wind energy data, used in Problem II, Problem III, and Problem IV, is obtained from EXIST transparency platform via the provided Application Programming Interface (API). Considering Gökçekaya PSPP unit size (350 MW), four major wind generation holding companies are taken as a basis [45]. Under operation, under construction, and licensed wind power plants of these holding companies are listed in Table C.1, Table C.2 and Table C.3, respectively. Moreover, prelicensed wind power plant capacities are shown in Table C.4. In order to simulate under construction, licensed, and prelicensed generation, operating power plants listed in Table C.5 are used. Power plants in this table are selected so that the total capacity is close to the sum of total

capacities in Table C.2, Table C.3, and Table C.4.

Finalized daily production plan of wind unit in transparency platform is treated as forecasted wind generation in the optimization problems. Forecasted generation of both selected and all wind units are separately gathered in an hourly resolution. On the other hand, actual generation of selected wind plants could not be directly obtained from the platform. For this reason, it is approximated by scaling actual generation of all wind plants with a ratio of forecasted generation of selected ones over forecasted generation of all wind plants in Turkey. It can be formulated as in Equation (3.1) as well. Forecasted and actual generation of selected wind plants are given as parameters to the optimization problems.

$$\begin{pmatrix} \textit{Actual Generation of} \\ \textit{Selected Wind Plants} \end{pmatrix} = \frac{\begin{pmatrix} \textit{Forecasted Generation of} \\ \textit{Selected Wind Plants} \end{pmatrix}}{\begin{pmatrix} \textit{Forecasted Generation of} \\ \textit{All Wind Plants} \end{pmatrix}} \begin{pmatrix} \textit{Actual Generation of} \\ \textit{All Wind Plants} \end{pmatrix} \tag{3.1}$$

3.1 Problem Formulation

Mixed integer linear programming, MILP, method is used in performing optimization due to its speed and efficiency. An algebraic modeling language, AMPL, is used to formulate the problem in a more flexible and efficient way [46]. With AMPL, one of the state-of-the-art solver, CPLEX, is used [47]. Optimization is performed on NEOS, which is a free cloud service that enables to solve optimization problems with various solver types [48, 49, 50]. Created optimization files are sent to NEOS servers via Extensible Markup Language-Remote Procedure Call Application Programming Interface (XML-RPC API). Results are obtained via XML-RPC API again and then processed.

In order to utilize MILP on the model, all objective functions and constraints should be linear. Equation (2.2) and Equation (2.9) in Chapter 2 are not suitable for MILP because they have three variables, which are flow rate, head and efficiency, in multi-

plication. After head is discretized and efficiency is piecewise linearized, power term becomes only a function of flow rate. Algorithms for the discretization of head levels and piecewise linearization of discharging model used in this dissertation are adapted from [19]. All constraints given below are common in all four problems. Constraints for the discretization are shown in Equation (3.2), (3.3), (3.4) and (3.5).

$$V_{u,t} \geqslant V_{u,L}(c_{1,t} - c_{2,t}) + V_{u,H}c_{2,t} \ , \forall t \in T \tag{3.2}$$

$$V_{u,t} \leqslant \bar{V_u}c_{2,t} + V_{u,L}(1 - c_{1,t}) + V_{u,H}(c_{1,t} - c_{2,t}) \ , \forall t \in T \tag{3.3}$$

$$c_{1,t} \geqslant c_{2,t} \ , \forall t \in T \tag{3.4}$$

$$\underline{V_u} \leqslant V_{u,t} \ , \forall t \in T \tag{3.5}$$

where $V_{u,t}$ (m^3) is upper reservoir water volume variable at time interval, t, and $\bar{V_u}$ (m^3), $\underline{V_u}$ (m^3) are upper and lower bounds of it, respectively. $V_{u,H}$ (m^3) and $V_{u,L}$ (m^3) are higher and lower limits used for volume level discretization. Finally, $c_{1,t}$ and $c_{2,t}$ are binary state variables which determines the discrete volume level at time interval, t.

When the upper volume is in the higher range, Equation (3.2) and (3.3) force $c_{1,t}$ and $c_{2,t}$ to become both 1. If the upper volume is in the medium range, then $c_{1,t}$ is forced to become 1 and $c_{2,t}$ is forced to become 0 by Equation (3.2) and (3.3). As a final possibility, if the upper volume is in the lower range, then Equation (3.2) and (3.3) forces $c_{1,t}$ and $c_{2,t}$ to become both 0. The constraint in Equation (3.4) prevents $c_{1,t}$ equaling 0 and $c_{2,t}$ equaling 1 at the same time interval, t. In other words, $c_{1,t}$ and $c_{2,t}$ both equaling 1, states volume is in the higher range. Otherwise, $c_{1,t}$ equaling 1 and $c_{2,t}$ equaling 0, states volume is in the medium range. Else, $c_{1,t}$ and $c_{2,t}$ both equaling 0, states volume is in the lower range. Lastly, the constraint in Equation (3.5) keeps the upper reservoir volume greater than or equal to $\underline{V_u}$.

The relation between upper reservoir water elevation and volume is shown in Figure 3.1. Because the curve in the figure is more close to a linear line, $V_{u,L}$ is set to 1/3 of the available volume, while $V_{u,H}$ is set to 2/3 of it, as shown in Equation (3.6) and (3.7), respectively. It should also be noted that the lower reservoir of Gökçekaya PSPP is almost 20 times larger than its upper reservoir as stated in Table 1.1. Thus, a change in water level of the lower reservoir is neglected due to its high reservoir volume and the short term horizon of the optimization.

$$V_{u,L} = \frac{(\bar{V_u} - \underline{V_u})}{3} \tag{3.6}$$

$$V_{u,H} = \frac{2(\bar{V_u} - \underline{V_u})}{3} \tag{3.7}$$

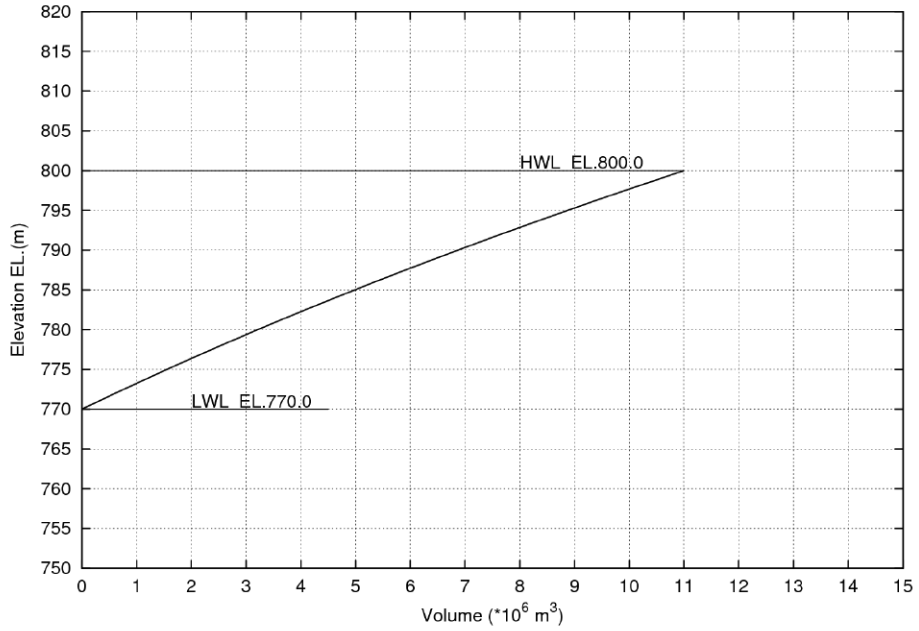

Figure 3.1: Storage Capacity Curve of the Upper Reservoir [11].

After discretization of head levels, operation curves are piecewise linearized for each level. Thanks to AMPL piecewise notation, piecewise equations can be written in a more clear way [46]. Basically, the expression shown below gives the piecewise linearized function of $vertical\ axis\ variable$.

$<< horizantal\ axis\ values\ of\ breakpoints; slopes >>$
$(horizantal\ axis\ variable, horizantal\ axis\ crossing\ point)$

Constraints in Equation (3.8) and Equation (3.9) shows the piecewise linearization of discharging at the lower head ($c_{1,t} = 0, c_{2,t} = 0$) in this notation.

$$(E_{d,t} - \bar{E_d}^L(c_{1,t} + c_{2,t}))- << Q^L_{d_1}..Q^L_{d_n}; s^L_{d_1}..s^L_{d_{n+1}} >> (Q_{d,t}, Q^L_{d_0}) \leqslant 0\ , \forall t \in T \tag{3.8}$$

$$(E_{d,t} + \bar{E_d}^L(c_{1,t} + c_{2,t}))- << Q^L_{d_1}..Q^L_{d_n}; s^L_{d_1}..s^L_{d_{n+1}} >> (Q_{d,t}, Q^L_{d_0}) \geqslant 0\ , \forall t \in T \tag{3.9}$$

where $\bar{E_d}^L$ is maximum discharged energy, $Q^L_{d_1}..Q^L_{d_n}$ are breakpoint discharge values, $s^L_{d_1}..s^L_{d_{n+1}}$ are slopes, and $Q^L_{d_0}$ is $Q\ axis$ crossing point of the trajectory line, all for lower head level. Because the first slope covers the values before the first breakpoint and the last slope covers the values after the last breakpoint, the number of slopes is one greater than the number of breakpoints. Illustration of these equations can be seen in Figure 3.2.

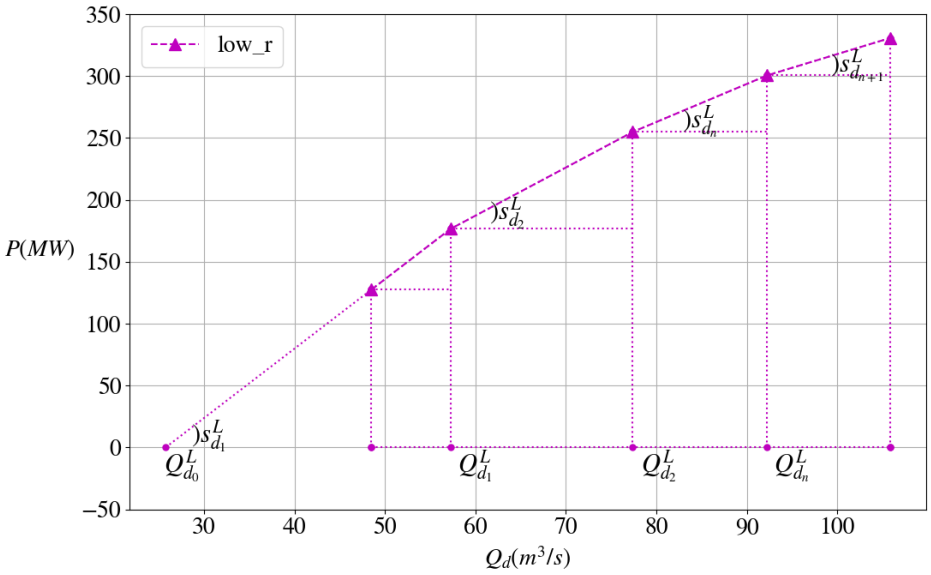

Figure 3.2: Piecewise Linear Function Discharging at Lower Head.

By utilizing binary variables $c_{1,t}$ and $c_{2,t}$, piecewise linearization of medium head level ($c_{1,t} = 1, c_{2,t} = 0$) can be expressed as in Equation (3.10) and Equation (3.11), whereas higher head level ($c_{1,t} = 1, c_{2,t} = 1$) can be represented as in Equation (3.12) and Equation (3.13).

$$(E_{d,t} - \bar{E_d}^M(1 - c_{1,t} + c_{2,t}))- << Q_{d_1}^M..Q_{d_n}^M; s_{d_1}^M..s_{d_{n+1}}^M >> (Q_{d,t}, Q_{d_0}^M) \leqslant 0 \ , \forall t \in T \tag{3.10}$$

$$(E_{d,t} + \bar{E_d}^M(1 - c_{1,t} + c_{2,t}))- << Q_{d_1}^M..Q_{d_n}^M; s_{d_1}^M..s_{d_{n+1}}^M >> (Q_{d,t}, Q_{d_0}^M) \geqslant 0 \ , \forall t \in T \tag{3.11}$$

$$(E_{d,t} - \bar{E_d}^H(2 - c_{1,t} - c_{2,t}))- << Q_{d_1}^H..Q_{d_n}^H; s_{d_1}^H..s_{d_{n+1}}^H >> (Q_{d,t}, Q_{d_0}^H) \leqslant 0 \ , \forall t \in T \tag{3.12}$$

$$(E_{d,t} + \bar{E_d}^H(2 - c_{1,t} - c_{2,t}))- << Q_{d_1}^H..Q_{d_n}^H; s_{d_1}^H..s_{d_{n+1}}^H >> (Q_{d,t}, Q_{d_0}^H) \geqslant 0 \ , \forall t \in T \tag{3.13}$$

where $\bar{E_d}^M$ and $\bar{E_d}^H$ are maximum discharged energy, $Q_{d_1}^M..Q_{d_n}^M$ and $Q_{d_1}^H..Q_{d_n}^H$ are breakpoint discharging values, $s_{d_1}^M..s_{d_{n+1}}^M$ and $s_{d_1}^H..s_{d_{n+1}}^H$ are slopes, $Q_{d_0}^M$ and $Q_{d_0}^H$ are $Q\ axis$ crossing points of the trajectory lines, for medium and higher head levels in discharging operation, respectively.

Pumping operation of the system can be expressed in a similar way to discharging operation. Equation (3.14) and Equation (3.15) shows pumping operation at lower head, Equation (3.16) and Equation (3.17) points pumping operation at medium head, Equation (3.18) and Equation (3.19) represents pumping operation at higher head.

$$(E_{p,t} - \bar{E_p}^L(c_{1,t} + c_{2,t}))- << Q_{p_1}^L..Q_{p_m}^L; s_{p_1}^L..s_{p_{m+1}}^L >> (Q_{p,t}, Q_{p_0}^L) \leqslant 0 \ , \forall t \in T \tag{3.14}$$

$$(E_{p,t} + \bar{E_p}^L(c_{1,t} + c_{2,t}))- << Q^L_{p_1}..Q^L_{p_m}; s^L_{p_1}..s^L_{p_{m+1}} >> (Q_{p,t}, Q^L_{p_0}) \geqslant 0\ , \forall t \in T \tag{3.15}$$

$$(E_{p,t} - \bar{E_p}^M(1 - c_{1,t} + c_{2,t}))- << Q^M_{p_1}..Q^M_{p_m}; s^M_{p_1}..s^M_{p_{m+1}} >> (Q_{p,t}, Q^M_{p_0}) \leqslant 0\ , \forall t \in T \tag{3.16}$$

$$(E_{p,t} + \bar{E_p}^M(1 - c_{1,t} + c_{2,t}))- << Q^M_{p_1}..Q^M_{p_m}; s^M_{p_1}..s^M_{p_{m+1}} >> (Q_{p,t}, Q^M_{p_0}) \geqslant 0\ , \forall t \in T \tag{3.17}$$

$$(E_{p,t} - \bar{E_p}^H(2 - c_{1,t} - c_{2,t}))- << Q^H_{p_1}..Q^H_{p_m}; s^H_{p_1}..s^H_{p_{m+1}} >> (Q_{p,t}, Q^H_{p_0}) \leqslant 0\ , \forall t \in T \tag{3.18}$$

$$(E_{p,t} + \bar{E_p}^H(2 - c_{1,t} - c_{2,t}))- << Q^H_{p_1}..Q^H_{p_m}; s^H_{p_1}..s^H_{p_{m+1}} >> (Q_{p,t}, Q^H_{p_0}) \geqslant 0\ , \forall t \in T \tag{3.19}$$

where $\bar{E_p}^L$, $\bar{E_p}^M$ and $\bar{E_p}^H$ are maximum pumped energy, $Q^L_{p_1}..Q^L_{p_m}$, $Q^M_{p_1}..Q^M_{p_m}$ and $Q^H_{p_1}..Q^H_{p_m}$ are breakpoint pumping values, $s^L_{p_1}..s^L_{p_{m+1}}$, $s^M_{p_1}..s^M_{p_{m+1}}$ and $s^H_{p_1}..s^H_{p_{m+1}}$ are slopes, $Q^L_{p_0}$, $Q^M_{p_0}$ and $Q^H_{p_0}$ are $Q\ axis$ crossing points of the trajectory lines, for lower, medium, and higher head levels in pumping operation, respectively. It can be noted that since the discretized pumping model is linear as described in Chapter 2, empty set of breakpoint pumping values and single slope defines the desired linear line.

3.1.1 Problem I: Maximization of Profit without Wind Energy

The objective of the problem is maximizing the profit in the day-ahead market for the PSPP. As stated before, wind energy is not considered in the optimization. The problem is solved in one day ahead (D-1) to plan the optimum hourly operation for the

next day (D). In this problem, the decision is made with a daily period. The objective function can be expressed as in Equation (3.20).

$$maximize \sum_{t=t_i}^{t_f} mcp_t(E_{d,t} - E_{p,t}) \ , \forall t \in T \tag{3.20}$$

where mcp_t $(\$)$ is a market clearing price at time interval, t. It is assumed that mcp_t is perfectly forecasted. Hence, it is given to the problem as a parameter for each hour. $E_{d,t}$ (MWh) and $E_{p,t}$ (MWh) are discharged and pumped energy at time interval, t. While discharged energy is sold to the market, pumped energy is bought from the market. Figure 3.3 shows the day-ahead planning algorithm when all constraints are satisfied.

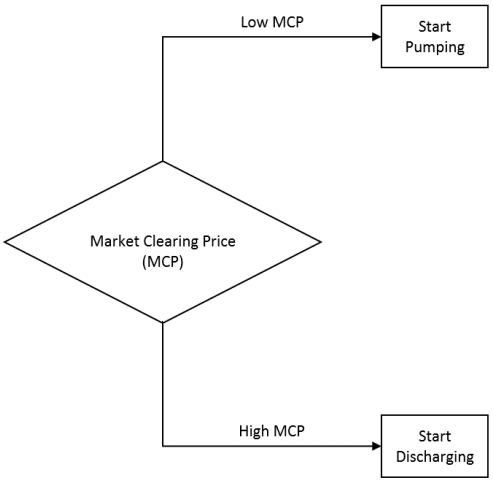

Figure 3.3: Day-ahead optimization algorithm for Problem I

Since it optimizes a day-ahead market problem, final time, t_f (h), is taken as 24 hours more than initial time, t_i (h), as shown in Equation (3.21).

$$t_f = t_i + 24 \tag{3.21}$$

Constraint in Equation (3.22) forces discharge rate, $Q_{d,t}$ (m^3/s), greater than or equal to minimum discharge rate, $\underline{Q}_d$ (m^3/s), when the system is discharging, i.e., discharg-

ing variable, d_t is 1.

$$d_t \underline{Q}_d \leqslant Q_{d,t} \ , \forall t \in T \tag{3.22}$$

Similarly, constraints in Equation (3.23) and Equation (3.24) keeps the $E_{d,t}$ in range, that is greater than or equal to minimum discharged energy $\underline{E}_d \ (MWh)$, and less than or equal to maximum discharged energy, $\bar{E}_d \ (MWh)$, when the PSPP is discharging.

$$d_t \underline{E}_d \leqslant E_{d,t} \ , \forall t \in T \tag{3.23}$$

$$E_{d,t} \leqslant d_t \bar{E}_d \ , \forall t \in T \tag{3.24}$$

Analogously, constraint in Equation (3.25) forces pump rate, $Q_{p,t} \ (m^3/s)$, greater than or equal to minimum pump rate, $\underline{Q}_p \ (m^3/s)$, when the system is pumping, i.e., pumping variable, p_t is 1.

$$p_t \underline{Q}_p \leqslant Q_{p,t} \ , \forall t \in T \tag{3.25}$$

In a similar manner, constraint in Equation (3.26) and Equation (3.27) keeps the $E_{p,t}$ in range, that is greater than or equal to minimum pumped energy $\underline{E}_p \ (MWh)$, and less than or equal to maximum pumped energy, $\bar{E}_p \ (MWh)$, when the PSPP is pumping.

$$p_t \underline{E}_p \leqslant E_{p,t} \ , \forall t \in T \tag{3.26}$$

$$E_{p,t} \leqslant p_t \bar{E}_p \ , \forall t \in T \tag{3.27}$$

Constraint in Equation (3.28) avoids the system discharging and pumping simultaneously at time interval, t.

$$p_t + d_t \leqslant 1 \ , \forall t \in T \tag{3.28}$$

Last but not least, constraint in Equation (3.29) satisfies the conservation of the upper reservoir volume for the next time step. Coefficient, 3600, converts second to an hour.

$$V_{u,t} = V_{u,t-1} + 3600(Q_{p,t-1} - Q_{d,t-1}) \ , \forall t \in T \tag{3.29}$$

3.1.2 Problem II: Maximization of Profit with Wind Energy

This problem has an objective to maximize the profit of PSPP and wind power plants cooperation. Different than Problem I, this problem takes cooperation with wind energy into account. The input energy for pumping is obtained from wind power plants instead of buying it from the market as in the previous problem. It is supposed that PSPP and wind plants operate in the same hypothetical portfolio. Similar to Problem I, Problem II makes a decision one day ahead (D-1), which is valid for the next 24 hours (D), on a daily basis. Objective function in Equation (3.20) needs to be updated. Sold wind energy to the market, $E_{w,t}$ (MWh), term should be added to the new objective function Equation (3.30). Sold wind energy is the net energy that is sold to the market.

$$maximize \sum_{t=t_i}^{t_f} mcp_t(E_{w,t} + E_{d,t} - E_{p,t}) \ , \forall t \in T \tag{3.30}$$

All constraints which belong to Problem I, are also valid for this problem. Moreover, two new constraint equations are introduced. The first one limits the upper bound of sold wind energy to the forecasted wind energy from day-ahead. In other words, planned sold wind energy can not exceed the forecasted wind energy as shown in Equation (3.31). The second constraint forces the system in a way that the source of the pumped energy should be the wind energy. That is to say, sum of the sold wind energy and pumped energy should be equal to forecasted wind energy as stated in Equation (3.32).

$$0 \leqslant E_{w,t} \leqslant E^f_{w,t} \ , \forall t \in T \tag{3.31}$$

$$E_{w,t} + E_{p,t} = E^{f}_{w,t} \, , \forall t \in T \tag{3.32}$$

where $E^{f}_{w,t}$ (MWh) is forecasted wind energy for all wind units in Table C.1 and Table C.5 at time interval, t.

3.1.3 Problem III: Minimization of Wind Energy Deviations

Unlike Problem I and Problem II, Problem III tries to minimizing wind energy deviations in balancing power market. Although balancing power market operates in real time, the resolution of time is set to an hour for the sake of simplicity. For this reason, optimization is run hourly for deciding the operation of each hour.

Because wind energy is forecasted one day ahead, there could be a forecasting error in actual generation. Wind energy deviation, $E^{d}_{w,t}$ (MWh), is nothing but subtracting forecasted wind energy, $E^{f}_{w,t}$ (MWh), from actual wind energy, $E^{a}_{w,t}$ (MWh), in the problem as shown in Equation (3.33).

$$E^{d}_{w,t} = E^{a}_{w,t} - E^{f}_{w,t}, \forall t \in T \tag{3.33}$$

A dummy variable, dif_t, is introduced to take the absolute value of the energy difference between $E^{d}_{w,t}$ and $(E_{p,t} - E_{d,t})$. Objective function minimizes this dummy variable as shown in Equation (3.34).

$$minimize \; dif_t \, , \forall t \in T \tag{3.34}$$

Constraints in Equation (3.35) and Equation (3.36) are introduced in this problem and they forces dif_t equals to $|E^{d}_{w,t} - (E_{p,t} - E_{d,t})|$.

$$dif_t \geqslant E^{d}_{w,t} - (E_{p,t} - E_{d,t}) \, , \forall t \in T \tag{3.35}$$

$$dif_t \geqslant -E^{d}_{w,t} + (E_{p,t} - E_{d,t}) \, , \forall t \in T \tag{3.36}$$

While all constraints are satisfied, optimization algorithm can be expressed as in Figure 3.4.

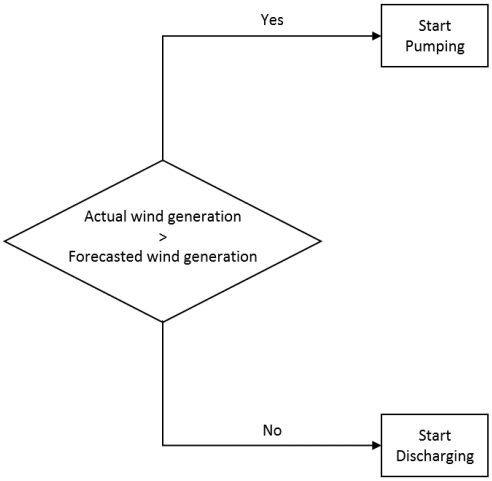

Figure 3.4: Real time optimization algorithm for Problem III

All constraints which belong to Problem I except the constraint in Equation (3.21), are valid for this problem, as well. Time resolution is set to an hour and, so constraint in Equation (3.21) should be updated as stated in Equation (3.37).

$$t_f = t_i + 1 \tag{3.37}$$

3.1.4 Problem IV: Maximization of Profit with Wind Energy and Minimization of Wind Energy Deviations

As its name implies, this problem is a combination of Problem II and Problem III. While maximizing the profit in day-ahead market is aimed, it also tries to minimize wind energy deviations in balancing power market by hourly manner. In other words, profit maximization problem is solved daily to plan the optimum operation of the following day. On the other hand, based on the wind forecast accuracy, corrective action on the operation plan is taken by solving the imbalance minimization problem in each hour.

For the day-ahead planning, this problem covers the objective function equation and

all constraint equations of Problem II, but there are some slight differences between them.

As a beginning, $\bar{V}_u$ and $\underline{V}_u$ should be updated so that, in case of a need in real time, it should not hit the actual limits. In other words, for flexible operation in the balancing power market, a safety margin in volume for day-ahead planning must be reserved. Two coefficients, which are upper safety margin coefficient for upper volume, $\bar{k}_{V_u}$, and lower safety margin coefficient for upper volume, $\underline{k}_{V_u}$, should be introduced for this reason. These coefficients are calculated by analyzing the wind energy imbalances. Energy imbalance due to the difference between actual generation and forecasted generation of wind plants is also called as mismatch in the problem. In order to consider the effect of consecutive mismatch, successive mismatches that have the same sign (direction) are summed between March 1st, 2018 to March 1st, 2019, for total wind generation in Turkey. The distribution of the successive sum mismatches can be seen in Figure 3.5.

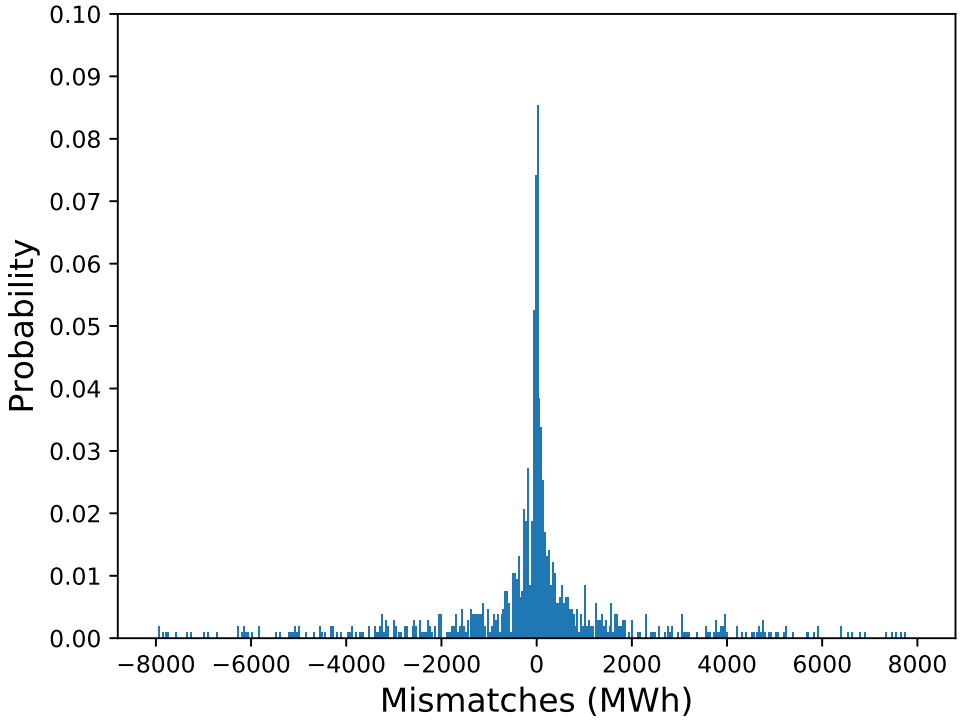

Figure 3.5: Distribution of Successive Sum Mismatches

Two ranges that covers 60% and 75% of distribution are calculated as [-760, 800] and [-1640, 1680], respectively. By scaling those ranges to the total wind installed capacity, $\bar{k}_{V_u}$ and $\underline{k}_{V_u}$ are found. The first range corresponds to 0.9 and 1.1 upper and lower safety margin coefficients, respectively, whereas the latter stands for 0.75 and 1.25. Hence, constraints in Equation (3.3) and Equation (3.5) should be updated as shown in constraints Equation (3.38) and Equation (3.39), respectively.

$$V_{u,t} \leqslant \bar{k}_{V_u} \bar{V}_u c_{2,t} + V_{u,L}(1 - c_{1,t}) + V_{u,H}(c_{1,t} - c_{2,t}) \ , \forall t \in T \tag{3.38}$$

$$\underline{k}_{V_u} \underline{V}_u \leqslant V_{u,t} \ , \forall t \in T \tag{3.39}$$

Furthermore, similar to the limitations on the volume, there should be safety margins for discharged energy and pumped energy limits. $\bar{k}_{E_d}$, $\underline{k}_{E_d}$, are upper and lower safety margin coefficients for discharged energy, while $\bar{k}_{E_p}$, $\underline{k}_{E_p}$ are safety margin coefficients for pumped energy. In this problem these coefficients are kept constant, where $\bar{k}_{E_d}$ and $\bar{k}_{E_p}$, are taken as 0.9 while $\underline{k}_{E_d}$ and $\underline{k}_{E_p}$, are taken as 1.1. By using these coefficients, constraints in Equation (3.23), Equation (3.24), Equation (3.26) and Equation (3.27) should be updated as in Equation (3.40), Equation (3.41), Equation (3.42) and Equation (3.43), respectively.

$$\underline{k}_{E_p} d_t \underline{E}_d \leqslant E_{d,t} \ , \forall t \in T \tag{3.40}$$

$$E_{d,t} \leqslant \bar{k}_{E_d} d_t \bar{E}_d \ , \forall t \in T \tag{3.41}$$

$$\underline{k}_{E_p} p_t \underline{E}_p \leqslant E_{p,t} \ , \forall t \in T \tag{3.42}$$

$$E_{p,t} \leqslant p_t \ \bar{k}_{E_p} \bar{E}_p \ , \forall t \in T \tag{3.43}$$

For the real time operation, this problem covers objective function equation and all

the constraints of Problem III. However, constraints in Equation (3.35) and (3.36) should be revised as in Equation (3.44) and Equation (3.45).

$$dif_t \geqslant E^d_{w,t} - ((E_{p,t} - E^{planned}_{p,t}) - (E_{d,t} - E^{planned}_{d,t})) \, , \forall t \in T \tag{3.44}$$

$$dif_t \geqslant -E^d_{w,t} + ((E_{p,t} - E^{planned}_{p,t}) - (E_{d,t} - E^{planned}_{d,t})) \, , \forall t \in T \tag{3.45}$$

where $E^{planned}_{d,t}$ and $E^{planned}_{p,t}$ are day-ahead planning outcomes for discharged and pumped energy which are parameters in the equation. Moreover, forecasted wind energy in Equation (3.31) and (3.32) need to be changed by actual wind energy as stated in Equation (3.46) and Equation (3.47).

$$0 \leqslant E_{w,t} \leqslant E^a_{w,t} \, , \forall t \in T \tag{3.46}$$

$$E_{w,t} + E_{p,t} = E^a_{w,t} \, , \forall t \in T \tag{3.47}$$

Now, volume and energy limits should be set back to their original values without applying safety margins. In other words, in real time operations, constraints in Equation (3.3), Equation (3.5), Equation (3.23), Equation (3.24), Equation (3.26) and Equation (3.27) are used instead of using Equation (3.38), Equation (3.39), Equation (3.40), Equation (3.41), Equation (3.42) and Equation (3.43), respectively.

While day-ahead planning optimization algorithm is the same with Figure 3.3, real time optimization algorithm is updated and can be seen in Figure 3.6.

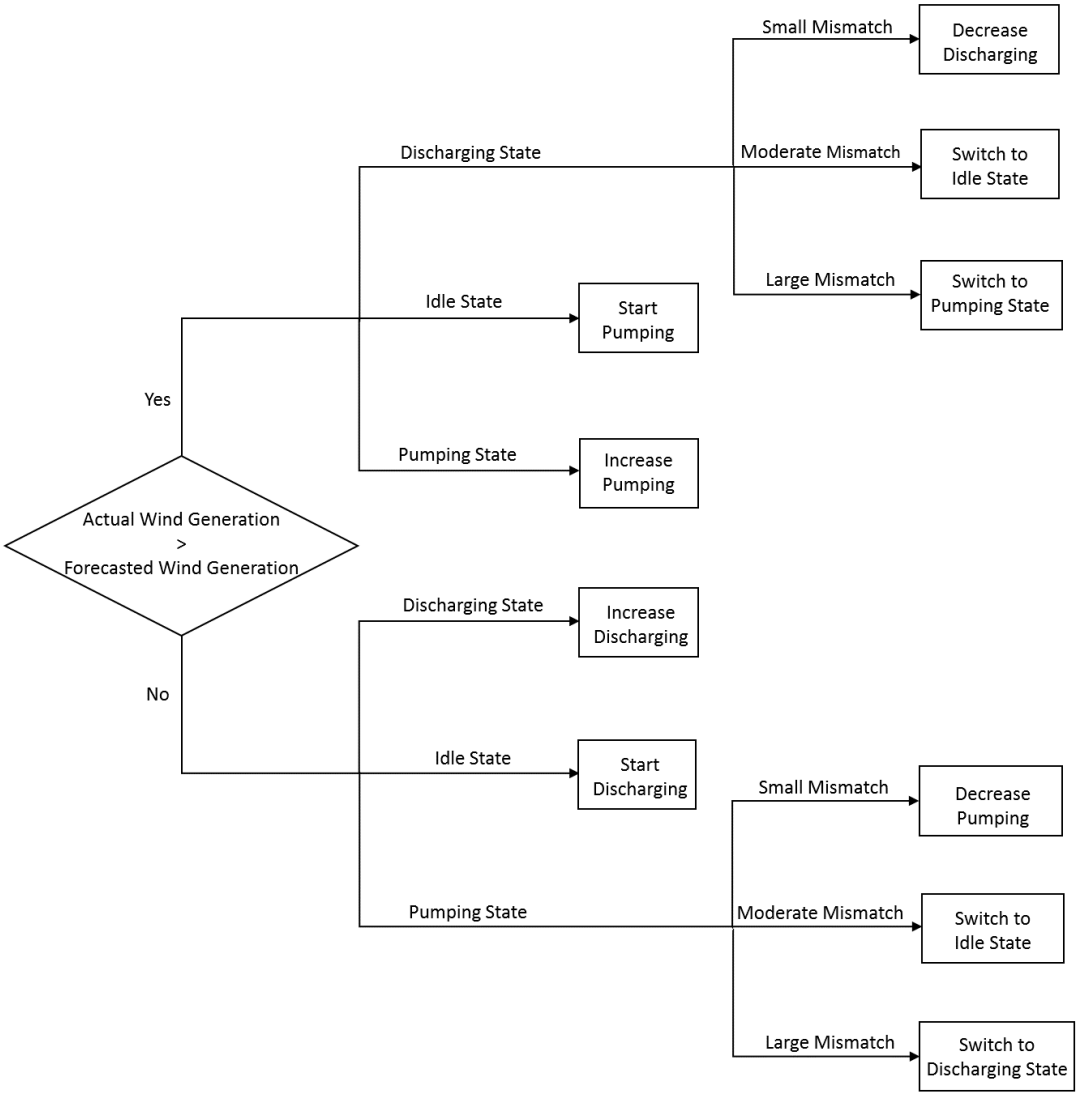

Figure 3.6: Real time optimization algorithm for Problem IV

It can be seen that the operation state in day-ahead planning may change depending on the energy imbalance direction and the magnitude. On the one hand, when there is excess wind energy, system may increase the pumping rate if it is already pumping. If the system was in idle state, it could switch to pumping state. When the system was planned to be in the discharging state, there are three possible scenarios based on the mismatch magnitude. If the imbalance is small, system decreases the discharging rate. For a moderate imbalance, system stops discharging and switches to the idle state. As the last option, large imbalances may switch system from the discharging

state to the pumping state. On the other hand, when there is a lack of wind energy, then system behaves in the same manner with the previous case. Discharging rate can increase if the system was already discharging. If the system was in the idle state, discharging could start. If it is planned to be pumping, system may decrease pumping, switch to idle state, switch to discharging state for small, moderate, large mismatches, respectively.

3.2 Conclusion

In the optimization problem, MILP method is implemented. Optimization is realized in AMPL language using CPLEX as a solver. Optimization problems are solved on NEOS servers. Moreover, market clearing price and forecasted wind energy data are obtained from EXIST transparency platform and fed to the problem as a parameter.

The Obtained model is utilized in four different short term control strategies. Problem I has an objective to maximize profit in day-ahead market by using PSPP alone. Problem II has the same target with Problem I. Different than Problem I, PSPP cooperates with wind plants in this problem. In Problem III, minimum wind energy imbalance is intended in real time by utilizing PSPP. The last problem has two objectives which are maximum profit in day-ahead market and minimum wind energy imbalance in real time. Optimization horizon is chosen 24 hour for Problem I, Problem II and Problem IV, while Problem III operates hourly.

CHAPTER 4

RESULTS AND DISCUSSIONS

In this chapter, simulation results of different optimization scenarios are presented. Although Gökçekaya PSPP has 4 x 350 MW units, only one of them is utilized in the optimization problem for the sake of simplicity. However, in order to examine the effect of a smaller pump unit, each of the problems introduced in Chapter 3, is also simulated for small pump unit cooperated with Gökçekaya reversible pump/turbine unit. One unit of Grimsel 2 PSPP, is chosen for a small unit due to similar operating head levels. Its operation range changes from 60 MW to 100 MW while pumping [51].

THe Initial volume of the upper reservoir, $V_{u,i}$, is taken as zero for all problems, except the Problem IV. For Problem IV, $V_{u,i}$ is set to its smallest value as expressed in Equation (3.39). Each problem is demonstrated by solving them consecutively for three days from December 31st, 2018 to January 2nd, 2019. Moreover, monthly analysis is run for August 2018 and January 2019.

4.1 Results for Problem I

Since the target for this problem is maximizing the profit in the day-ahead market, operation of the system strongly depends on the market clearing price. When the market clearing price is low enough, then energy is bought from the market and the system stores the energy by pumping water to upper volume. On the contrary, if the price is high enough, then the system discharges the water and sells the produced energy. For the medium price, system may stay in idle position. Moreover, since the optimization horizon is one day, the upper reservoir tends to remain empty at the end

of each 24 hours. Because there is no available water at the beginning of the day, system tries to fill the upper reservoir at the first time slot when the market clearing price is low.

Figure 4.1 shows upper reservoir water volume, discharged energy, pumped energy, market clearing price, turbine/pump efficiency, discharge flow rate and pump flow rate change with respect to time of Problem I and 1 turbine - 1 pump setup. As can be seen in the figure, market clearing price is low at hours 01:00-05:00 for day-1, so pumping mode is active for these hours. Contrariwise, the price is high at hours 07:00-22:00 for day-1. However, system is discharging only at 12:00 and 15:00-18:00 due to water limitation in upper reservoir. At hours 11:00-15:00 (35-39) for day-2, price is medium, and system is in idle state.

Figure 4.2 shows the case with 1 turbine - 2 pumps setup. It includes similar plots with Figure 4.1. The difference is that pumped energy and pumped flow rate subplots include the contribution from the smaller pump. This time, with the help of a small pump unit, system can pump more energy while the price is lower. As a result, much more energy can be sold while market clearing price is higher.

Monthly results for Problem I are given in Table 4.1. Total profit is the multiplication of market clearing price with the energy difference between discharged and pumped energy. It can be seen that additional pump unit increased the total profit. Furthermore, it can be noted that the total profit in August is much less than in January. A More stable market clearing price trend in August is the reason for this difference.

Table 4.1: Monthly Results for Problem I

		January	August
1 Turbine 1 Pump	Total Profit (USD)	1,701,737	322,244
1 Turbine 2 Pumps	Total Profit (USD)	2,074,489	407,271

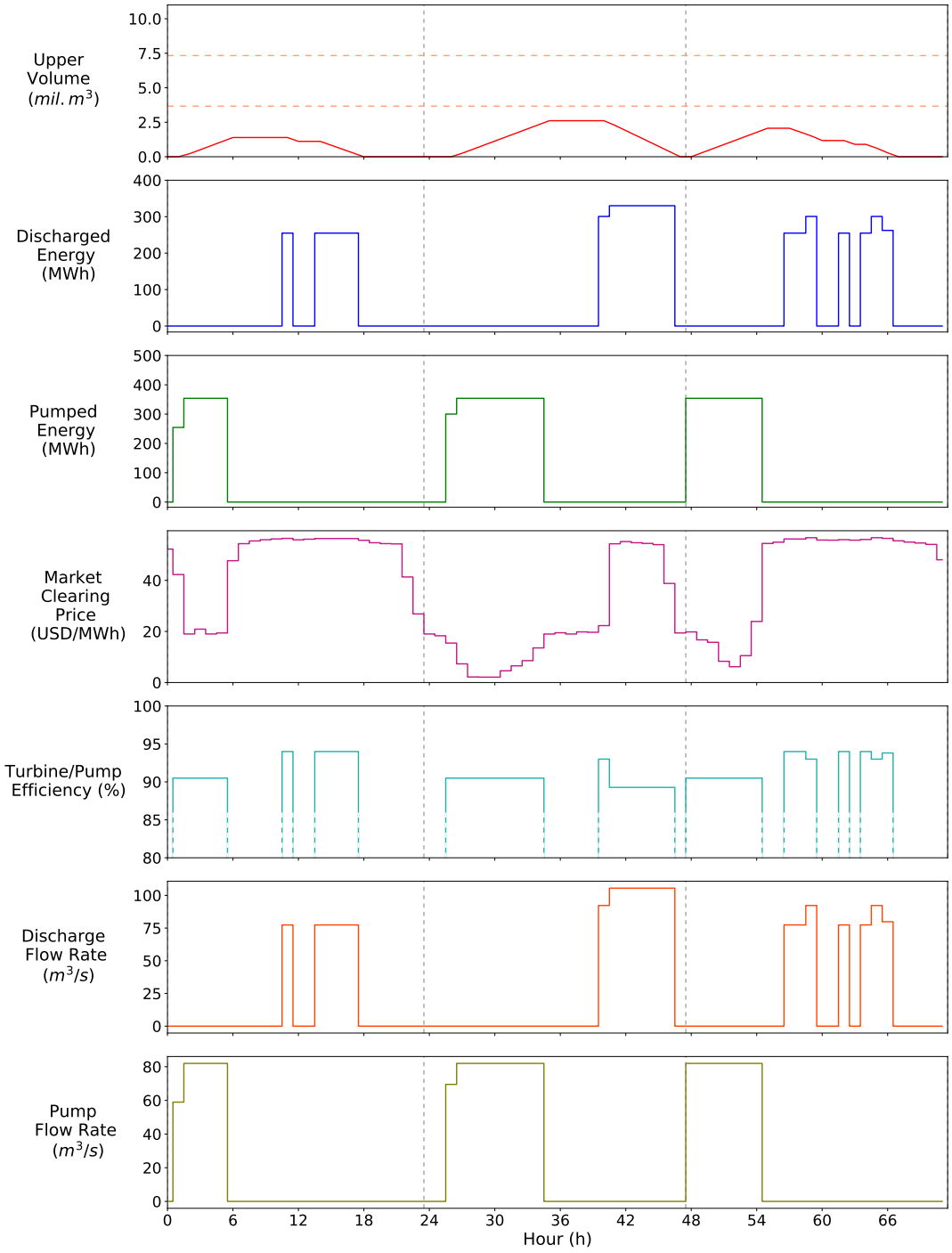

Figure 4.1: Problem I for 1 Turbine - 1 Pump Setup

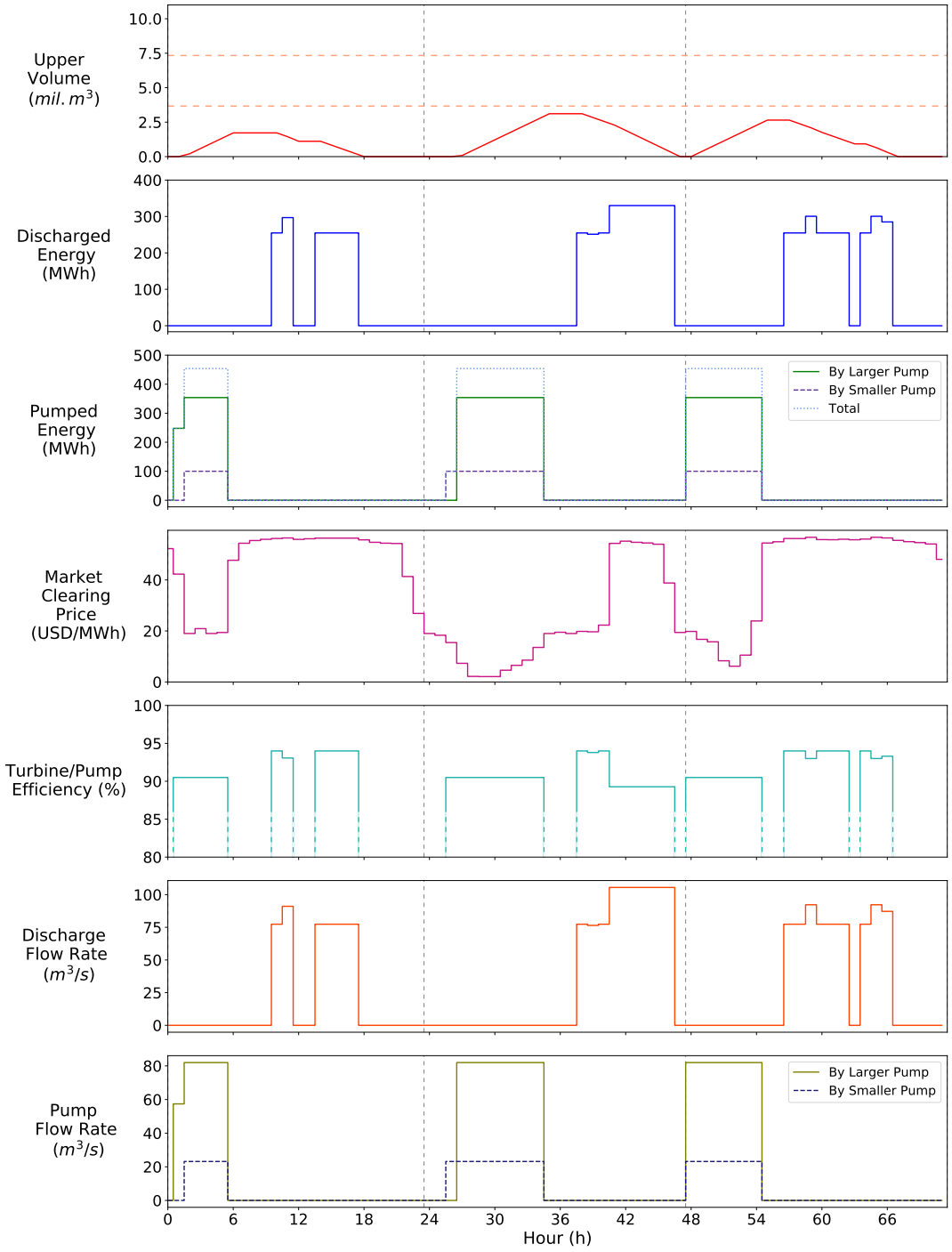

Figure 4.2: Problem I for 1 Turbine - 2 Pumps Setup

4.2 Results for Problem II

Owing to the fact that day-ahead planning of this problem is similar to the Problem I, results are also alike. Once the price is low, system tends to pump, whereas once the price is high system tends to discharge. However at this time, energy of pumping is transferred from wind power plants instead of day-ahead market. Figure 4.3 shows all plots of Problem II with 1 turbine - 1 pump setup. In addition to Figure 4.1, Figure 4.3 shows wind energy change with respect to time, as well. Forecasted wind energy is shown with a dashed line, while, wind energy which is planned to be sold to the market is shown with a solid line. It can be noted that planned to be sold wind energy follows the forecasted wind energy except the hours when the system is in the pumping state. For those hours, planned to be sold wind energy drops with a magnitude of pumped energy.

Furthermore, Problem II is examined for 1 turbine - 2 pumps setup, whose plots are given in Figure 4.4. Different than Figure 4.3, contribution of smaller pump is included in pumped energy and pump flow rate subplots in Figure 4.4. It should be emphasized that the small pump unit again supports the system while in pumping state.

Table 4.2 shows the monthly results for Problem II. Profit from PSPP is nothing but the multiplication of discharged energy and market clearing price. Since pumped energy is supplied from wind energy, it is not included in the expression. Profit from wind is the product of market clearing price and the remaining energy after subtracting pumped energy from forecasted wind energy. While this problem does not consider wind energy imbalances, total imbalance cost and total imbalance magnitude are given for the sake of completeness. Imbalance magnitude is the sum of absolute values of the difference between actual and forecasted wind energy. Imbalance cost will be explained in Section 4.4. Total profit is obtained by summing imbalance cost with profit from PSPP and wind. Although total profit in August is higher than in January, it can be seen that a larger part of the total profit comes from wind energy profit. Due to the fluctuated market clearing price, January has a higher profit from PSPP.

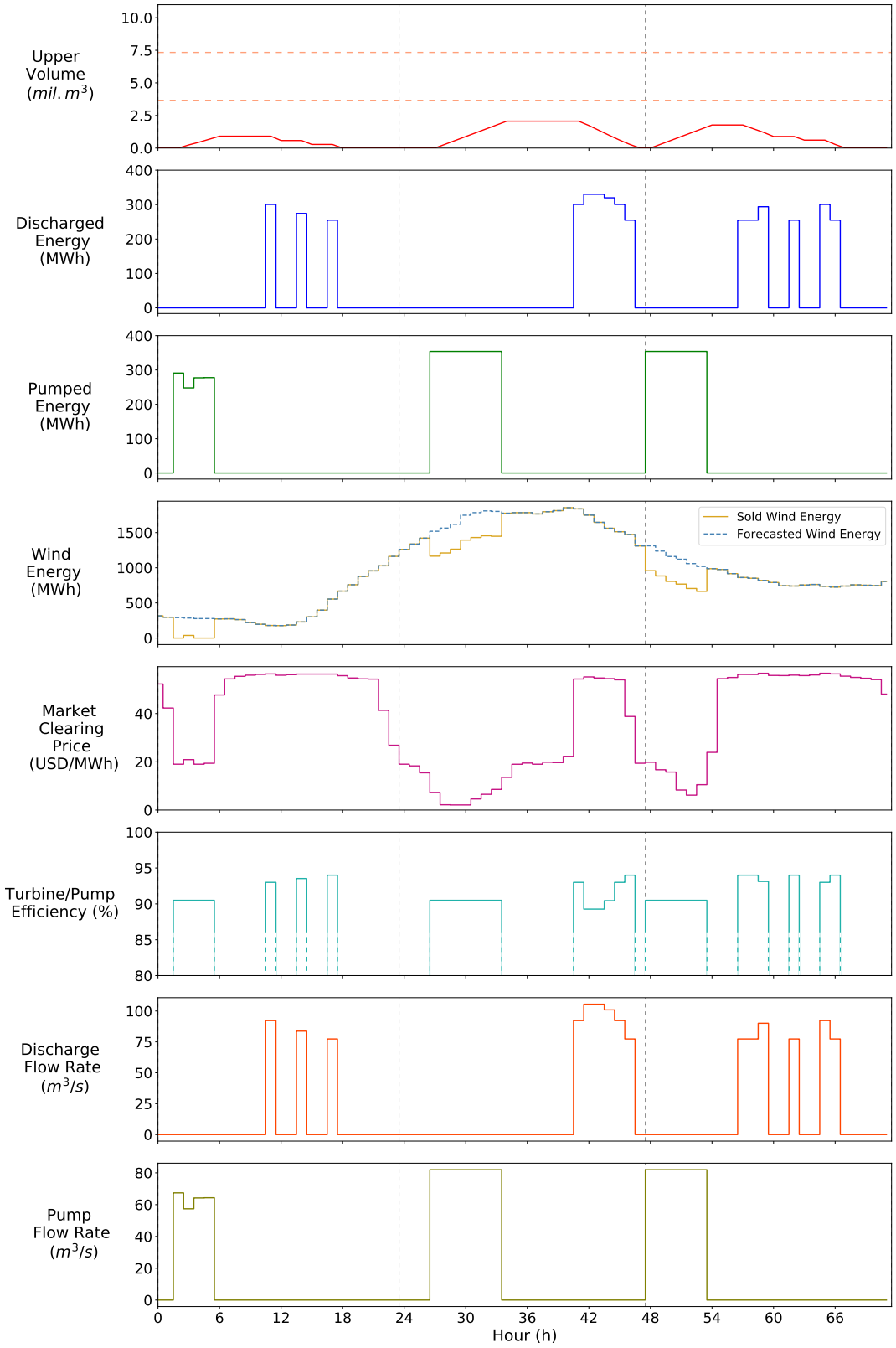

Figure 4.3: Problem II for 1 Turbine - 1 Pump Setup

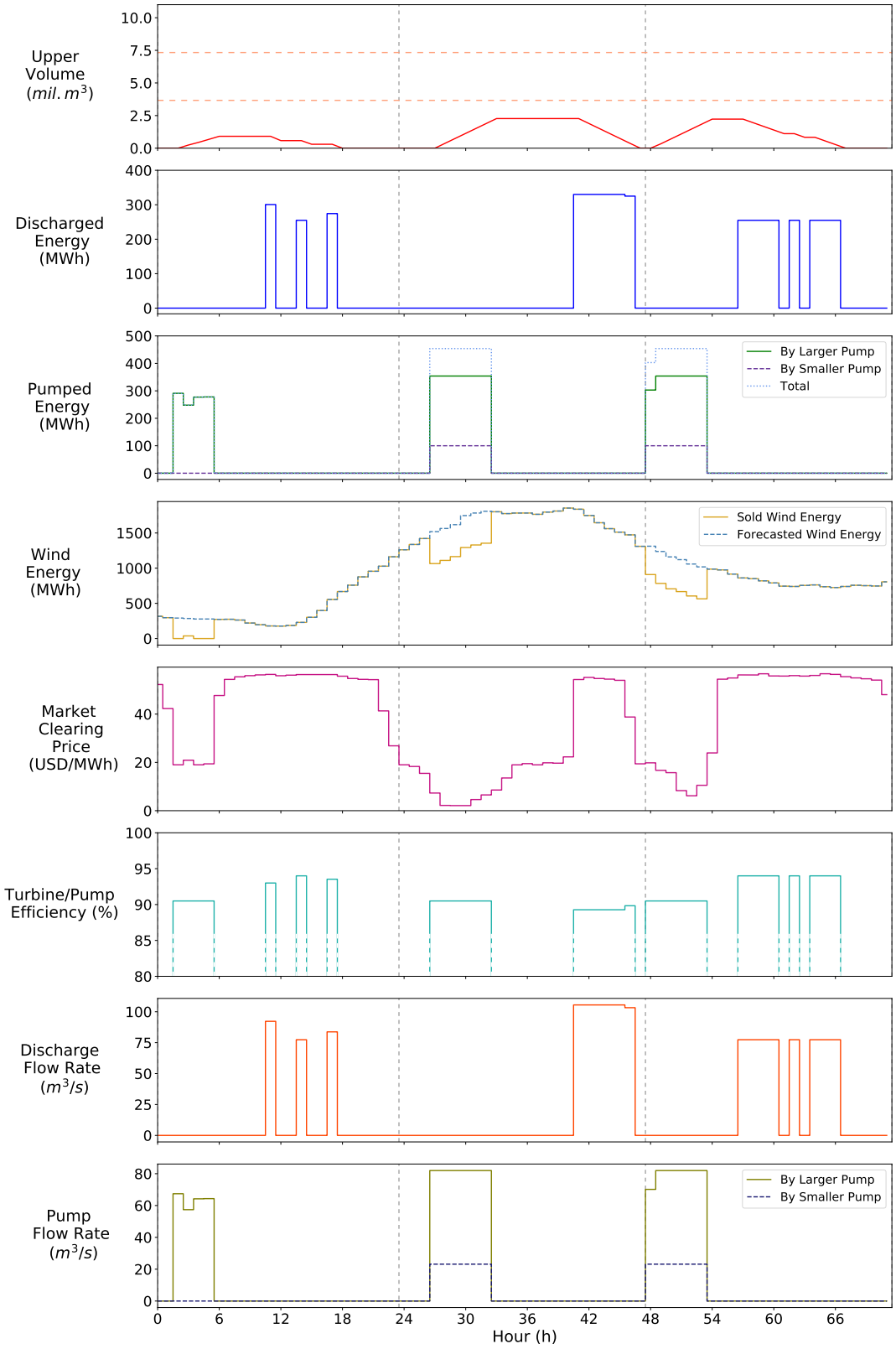

Figure 4.4: Problem II for 1 Turbine - 2 Pumps Setup

Table 4.2: Monthly Results for Problem II

		January	August
1 Turbine 1 Pump	Profit From PSPP (USD)	1,444,301	101,573
	Profit From Wind (USD)	44,506,890	61,038,060
	Imbalance Cost (USD)	-845,979	-602,415
	Imbalance Magnitude (MWh)	86,022	59,090
	Total Profit (USD)	45,105,213	60,537,218
1 Turbine 2 Pumps	Profit From PSPP (USD)	1,777,524	108,602
	Profit From Wind (USD)	44,437,699	61,034,977
	Imbalance Cost (USD)	-845,979	-602,415
	Imbalance Magnitude (MWh)	86,022	59,090
	Total Profit (USD)	45,369,244	60,541,164

4.3 Results for Problem III

Due to the fact that this problem aims minimizing the wind energy differences between actual and forecasted, results are quite different compared to Problem I or Problem II. Now, system operates in balancing power market in hourly real time. If the actual wind energy is more than forecasted wind energy, the system is pumping to compensate for the difference between them. On the other side, the actual wind energy is less than the forecasted one, then system discharges to complement the actual wind energy.

Figure 4.5 shows plots of Problem III for 1 turbine - 1 pump setup. It consists of the operation of system with upper volume, discharged energy, pumped energy, actual/-forecasted wind energy and before/after optimized energy difference, turbine/pump efficiency, discharge flow rate and pump flow rate plots with respect to time. It can be observed that actual wind energy is less than forecasted wind energy until 16:00 for day-1. If the upper reservoir was not empty for these hours, system would discharge to compensate for the negative energy mismatch. After 16:00 for day-1, actual wind energy becomes larger, and system pumps to minimize excess energy. When the en-

ergy difference is not enough to start pumping or discharging, system stays in idle position as at hours 17:00-19:00 (41-43) for day-2. System is in discharging state at hours 20:00-22:00 (44-46) for day-2 due to the negative wind energy imbalance.

Result of problem III for 1 turbine - 2 pumps setup is shown in Figure 4.6. Unlike the previous case, smaller mismatches can be compensated with the help of an additional small pump. As an example, at hours 18:00 for day-1 and 16:00-17:00 (40-41) for day-2 smaller pump worked and reduced the energy difference.

Monthly results for Problem III can be seen in Table 4.3. Calculation of imbalance magnitude is the same as the one in Table 4.2. It can be noted that thanks to the additional pump unit, the total imbalance magnitude decreased for both months.

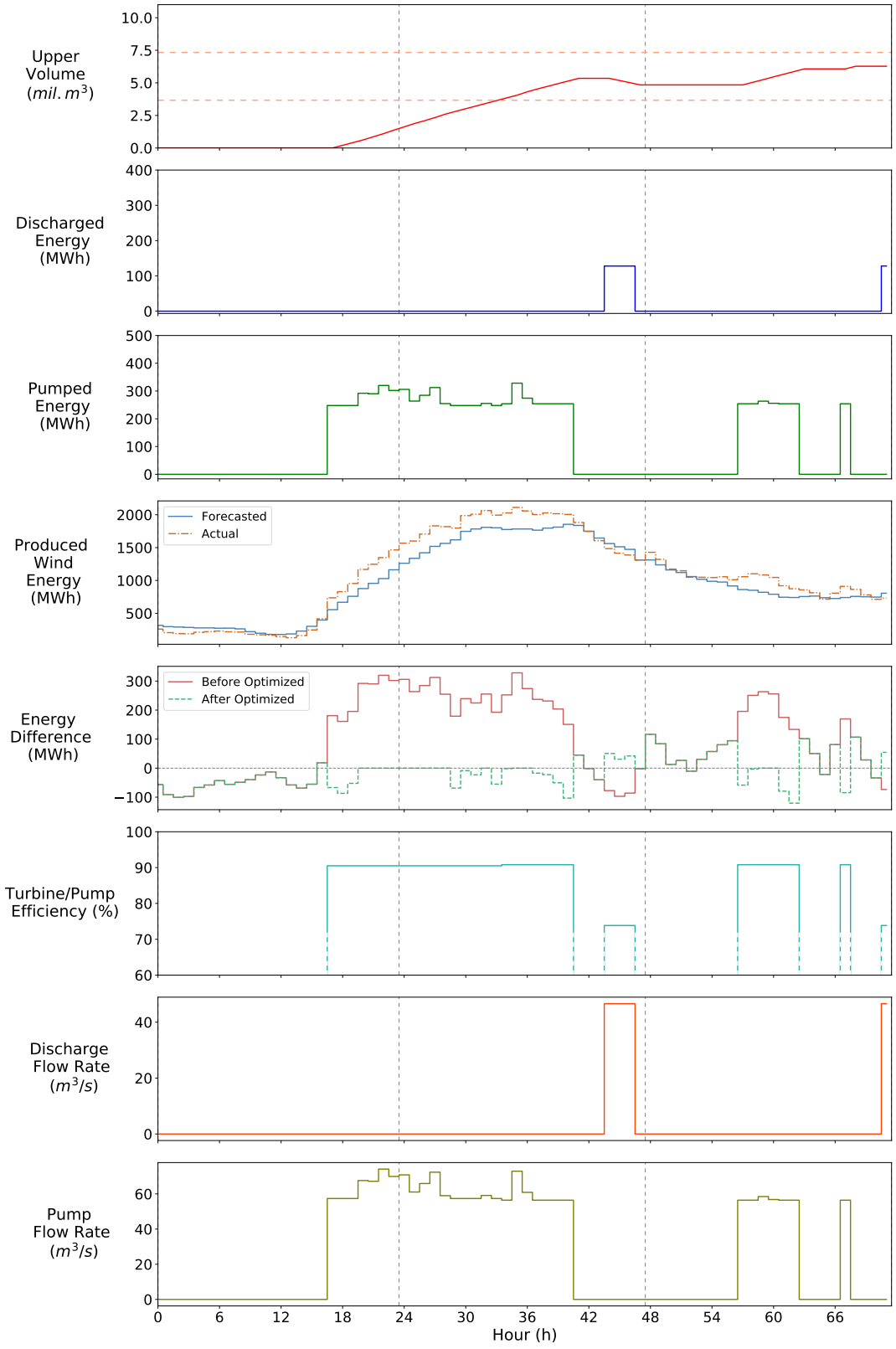

Figure 4.5: Problem III for 1 Turbine - 1 Pump Setup

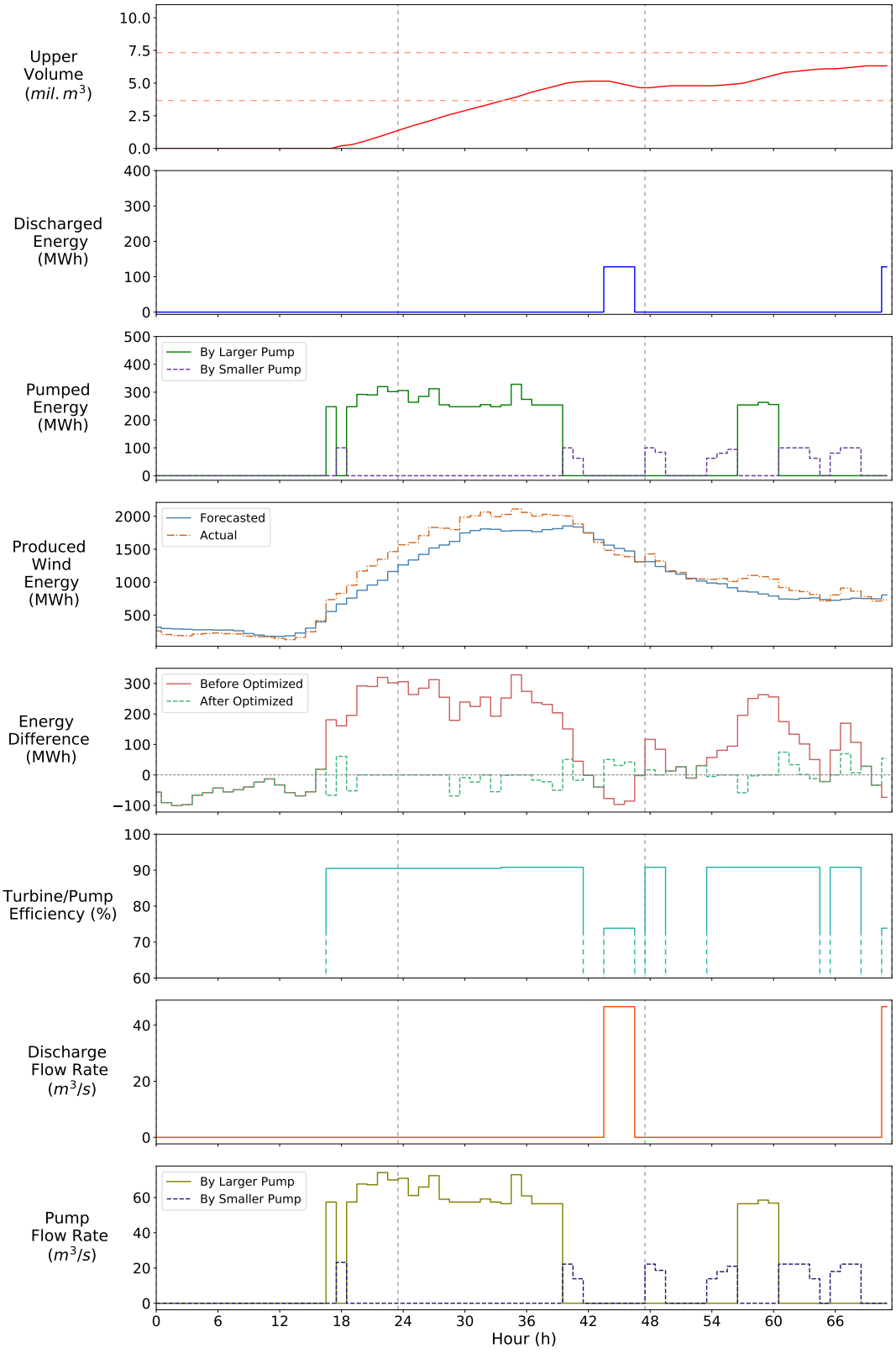

Figure 4.6: Problem III for 1 Turbine - 2 Pumps Setup

Table 4.3: Monthly Results for Problem III

		January	August
1 Turbine 1 Pump	Before Optimized Imbalance Magnitude (MWh)	86,022	59,090
	After Optimized Imbalance Magnitude (MWh)	45,196	42,749
1 Turbine 2 Pumps	Before Optimized Imbalance Magnitude (MWh)	86,022	59,090
	After Optimized Imbalance Magnitude (MWh)	31,177	28,721

4.4 Results for Problem IV

As stated in Chapter 3, this problem has two objectives. One of them is maximizing the profit in day-ahead market. The other one is minimizing the wind energy mismatches in balancing power market.

Figure 4.7 shows plots of Problem IV for 1 turbine - 1 pump setup when $\bar{k}_{V_u}$ and $\underline{k}_{V_u}$ are taken as 0.9 and 1.1, respectively. The figure includes day-ahead planned and real time optimized series for upper reservoir water volume, discharged energy, pumped energy, sold wind energy to the market, turbine/pump efficiency, discharge flow rate and pump flow rate with respect to time. Actual/forecasted wind energy, before/after optimized energy difference, market clearing price change with respect to time are also shown in the figure.

For the positive mismatches, i.e., actual wind energy is more than forecasted, plots can be analyzed based on planned system states. If the system is already in pumping state, then system tends to increase pumping as at hours 03:00-08:00 (27-32) for day-2. Otherwise, if the system is planned to be in idle state, then pumping operation starts to compensate mismatches as at hours 18:00-23:00 for day-1. Finally, if the system is discharging, then system tends to decrease discharging as at hours 08:00-09:00 (56-57) for day-3. If the mismatch is large enough system switch to idle state

as at hour 17:00 for day-1. When there are larger mismatches, system even switches to pumping state, but in this time frame there is no example for it.

In a similar way, for the negative mismatches, the figure can be analyzed per planned state. If the system is already discharging, then system needs to increase discharging as at hour 18:00-22:00 (42-46) for day-2. For the other case, if the system is in idle state, then discharging should start as at hours 03:00-04:00 for day-1. As a last case, when the system is planned to be in pumping state, system may decrease pumping, switch to idle state or even switch to discharging state depending on the magnitude of the mismatch. As an example, system switched to the idle state at hour 02:00 for day-1.

Figure 4.8 and Figure 4.9 show the results for Problem IV for 1 turbine - 2 pumps setup when $\bar{k}_{V_u}$ and $\underline{k}_{V_u}$ are taken as 0.9 and 1.1, respectively. Pumped energy plot in the figure shows the sum of pumped energy from larger and smaller pumps. It is noteworthy that optimized energy difference is more flat and close to zero line with the help of a smaller pump.

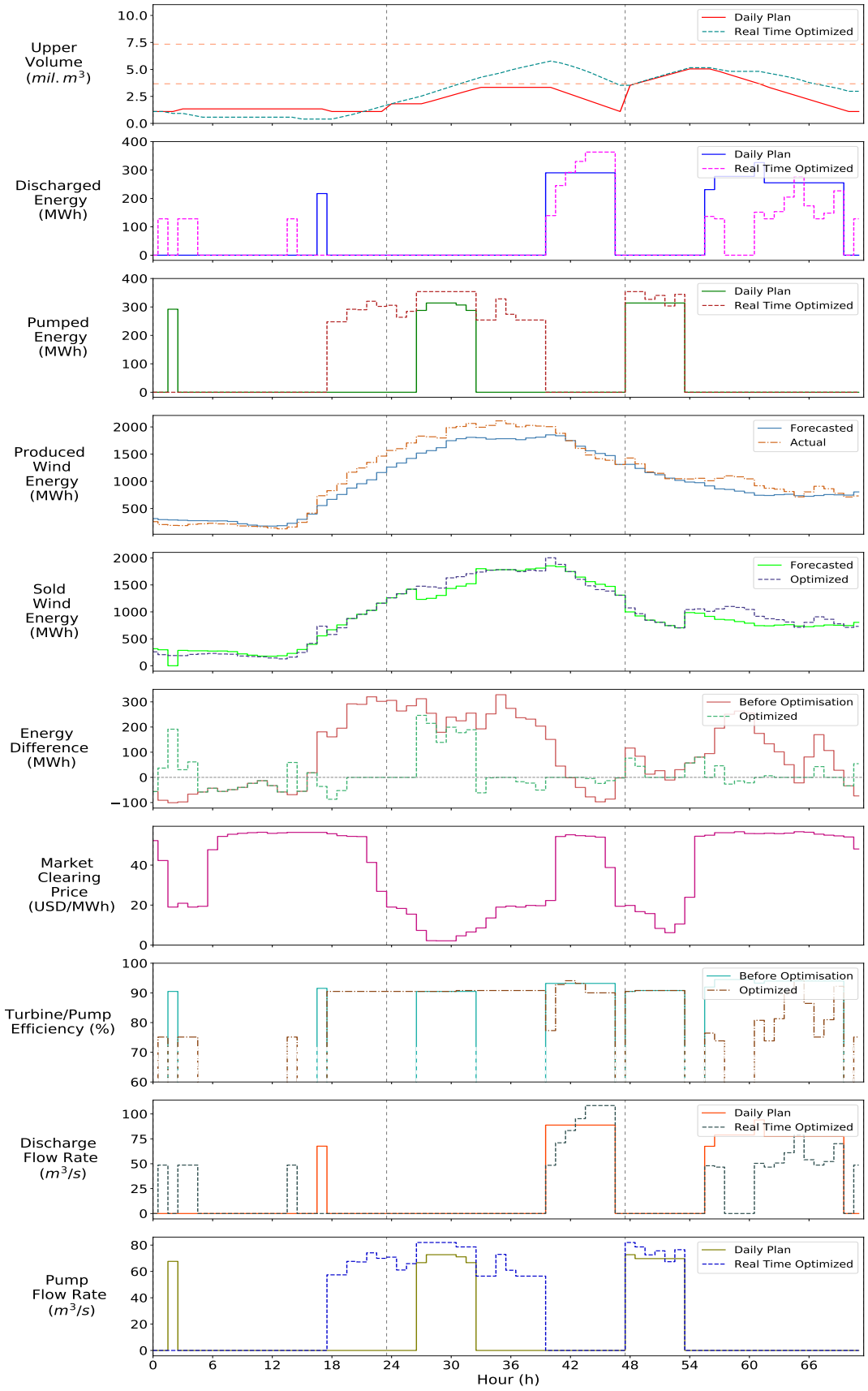

Figure 4.7: Problem IV for 1 Turbine - 1 Pump Setup for $\bar{k}_{V_u} = 0.9$ and $\underline{k}_{V_u} = 1.1$

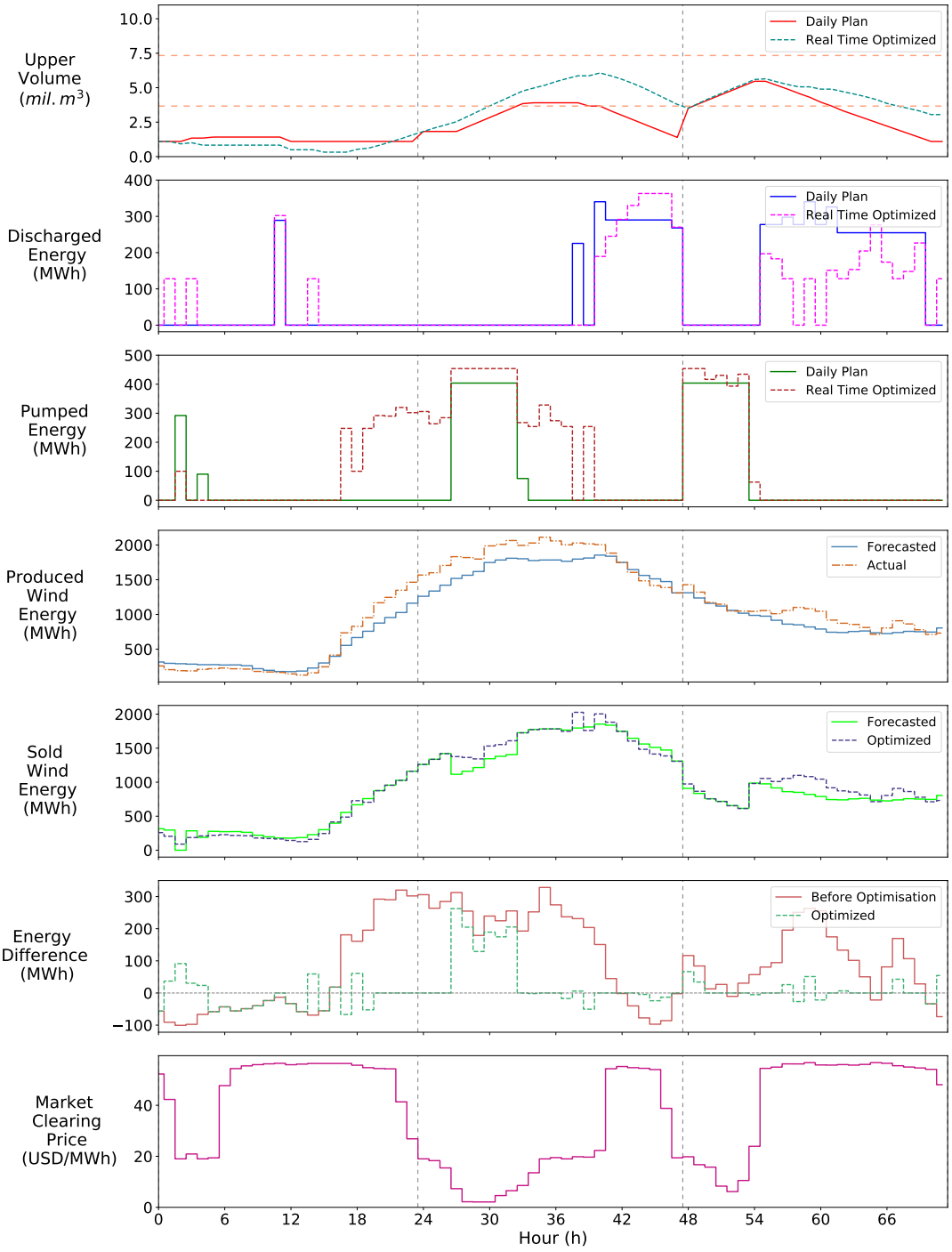

Figure 4.8: Problem IV for 1 Turbine - 2 Pumps Setup for $\bar{k}_{V_u} = 0.9$ and $\underline{k}_{V_u} = 1.1$ (Part I)

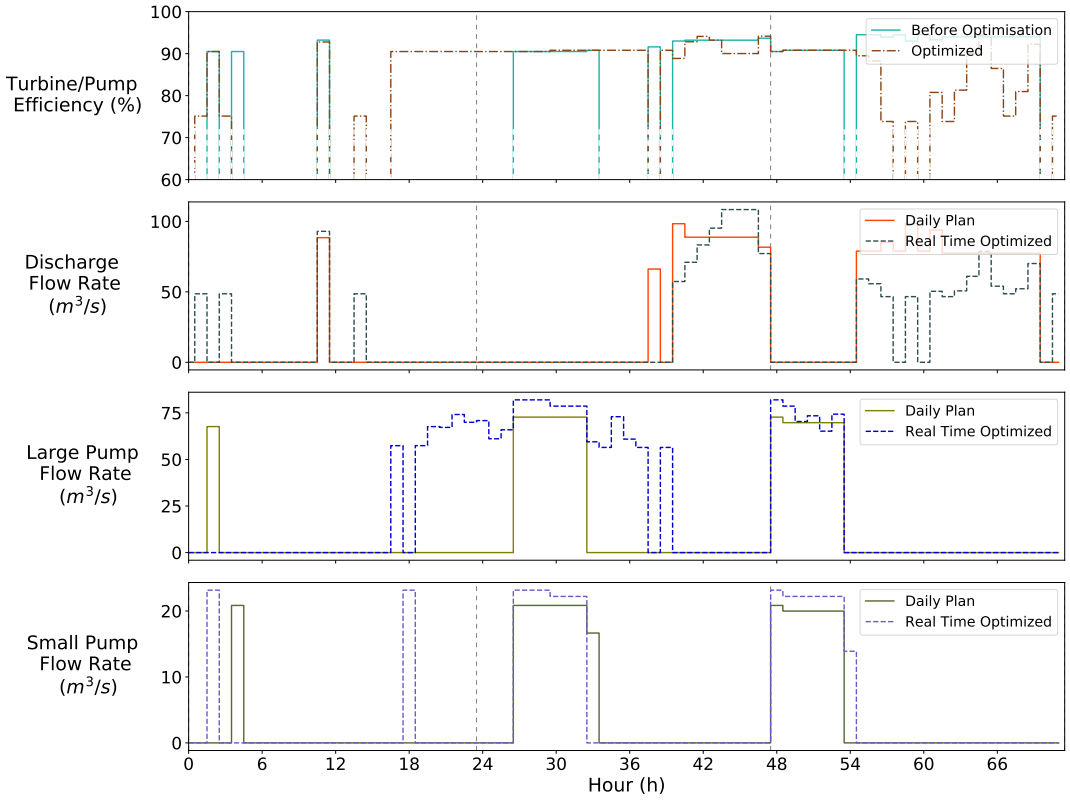

Figure 4.9: Problem IV for 1 Turbine - 2 Pumps Setup for $\bar{k}_{V_u} = 0.9$ and $\underline{k}_{V_u} = 1.1$ (Part II)

Figure 4.10 and Figure 4.11 show the results for Problem IV for 1 turbine - 2 pumps setup when $\bar{k}_{V_u}$ and $\underline{k}_{V_u}$ are taken as 0.75 and 1.25, respectively. It can be seen that initial upper volume is higher for this case. For day-ahead planning, system aims to be at least at this level. With having a larger margin, system is more flexible to compensate wind energy differences in real time.

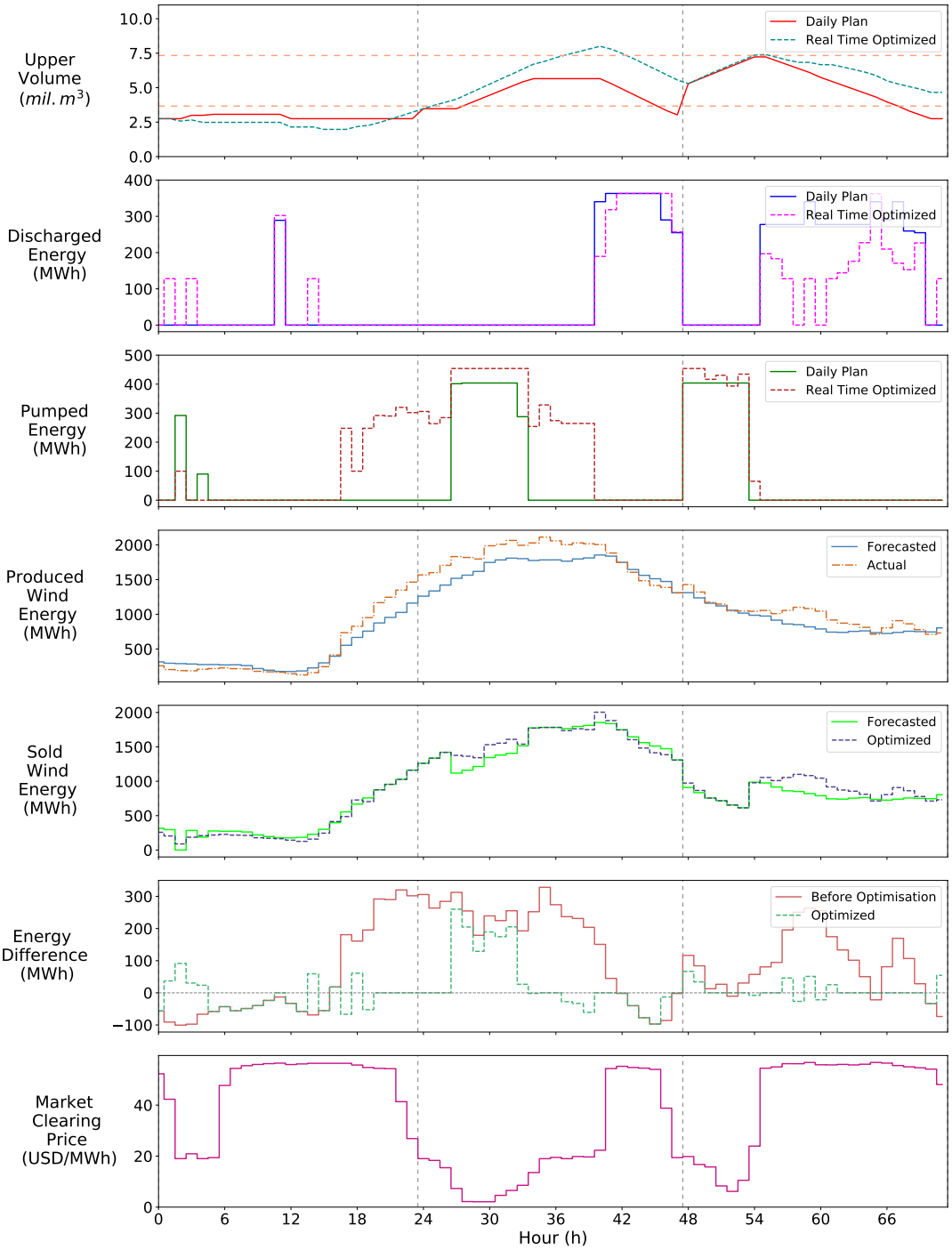

Figure 4.10: Problem IV for 1 Turbine - 2 Pumps Setup for $\bar{k}_{V_u} = 0.75$ and $\underline{k}_{V_u} = 1.25$ (Part I)

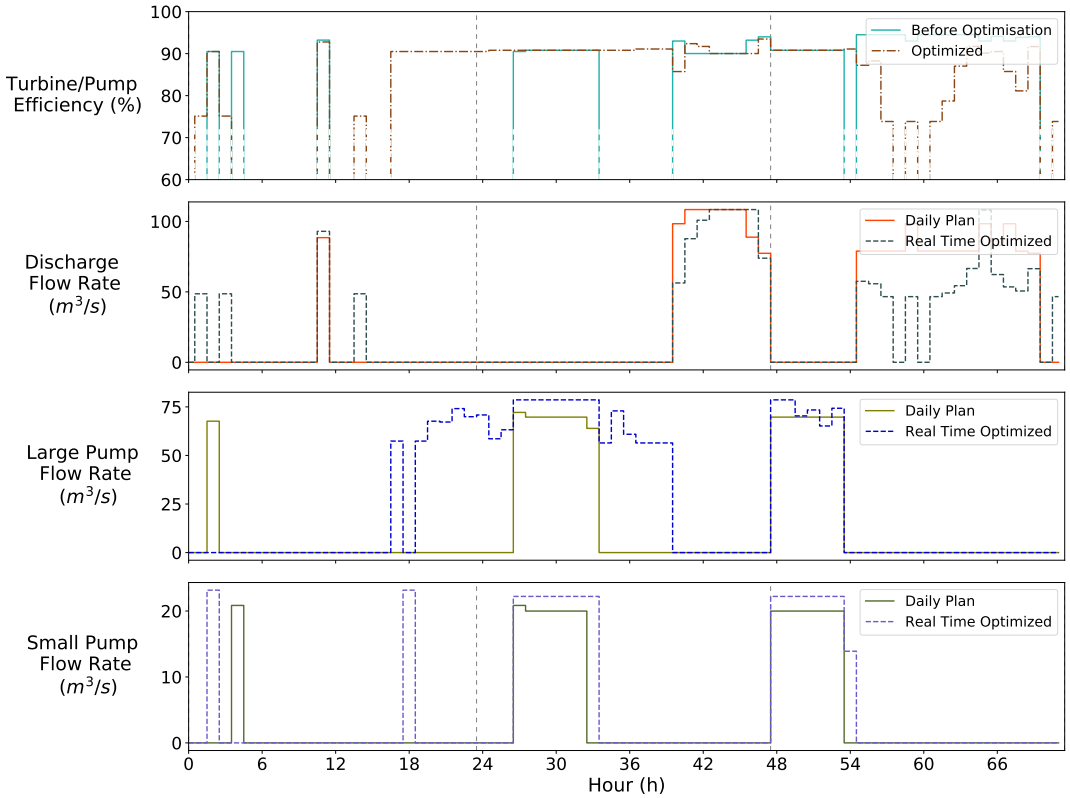

Figure 4.11: Problem IV for 1 Turbine - 2 Pumps Setup for $\bar{k}_{V_u} = 0.75$ and $\underline{k}_{V_u} = 1.25$ (Part II)

Monthly results for Problem IV are shown in Table 4.4. Total imbalance cost is obtained by summing hourly imbalance costs. Hourly imbalance cost is calculated by multiplying hourly imbalance energy with corresponding imbalance price. If the sign of the imbalance is positive, imbalance price is calculated by multiplication of 0.97 with a minimum of market clearing price and system marginal price. Otherwise, if the sign of the imbalance is negative, imbalance price is calculated by multiplication of 1.03 with a maximum of market clearing price and system marginal price. In this problem, imbalance magnitude is obtained after real time optimization. For both months, it can be seen that imbalance cost and magnitude decrease with 2 pumps setup with the help of smaller pump. Moreover, setup with wide safety margin coefficients has the lowest imbalance cost and magnitude. Because of this fact, the maximum total profit is obtained from this setup.

Table 4.4: Monthly Results for Problem IV

		January	August
1 Turbine 1 Pump $\bar{k}_{V_u} = 0.9$ $\underline{k}_{V_u} = 1.1$	Profit From PSPP (USD)	1,858,943	876,315
	Profit From Wind (USD)	44,357,685	60,248,585
	Imbalance Cost (USD)	-1,335,366	-1,373,939
	Imbalance Magnitude (MWh)	48,413	50,440
	Total Profit (USD)	44,881,262	59,750,961
1 Turbine 2 Pumps $\bar{k}_{V_u} = 0.9$ $\underline{k}_{V_u} = 1.1$	Profit From PSPP (USD)	2,095,654	688,011
	Profit From Wind (USD)	44,347,677	60,460,198
	Imbalance Cost (USD)	-1,311,958	-738,160
	Imbalance Magnitude (MWh)	37,833	26,244
	Total Profit (USD)	45,131,374	60,410,049
1 Turbine 2 Pumps $\bar{k}_{V_u} = 0.75$ $\underline{k}_{V_u} = 1.25$	Profit From PSPP (USD)	2,093,903	712,695
	Profit From Wind (USD)	43,903,478	59,423,503
	Imbalance Cost (USD)	-779,585	-186,186
	Imbalance Magnitude (MWh)	29,991	19,057
	Total Profit (USD)	45,217,796	60,541,164

4.5 Conclusion

In this chapter, optimization problems introduced in Chapter III are applied to Gökçekaya PSPP. Three day operation patterns are plotted and one month analysis results are tabulated for both August 2018 and January 2019.

Three day PSPP operation patterns are similar for Problem I and Problem II since they have the same aim. However, in Problem II, wind energy is utilized differently than Problem I. When the market clearing price is low, all produced wind energy is not sell to the market but instead some portion of it stored in PSPP as a potential energy to sell when the price is high. PSPP and wind plants operate in the same hypothetical portfolio. Hence, although the total profit in Problem I is higher than the profit from PSPP in Problem II, it is aimed to maximize the total profit of the

portfolio in Problem II. Problem III results in an increasing trend of upper reservoir volume due to positive mismatches, which is opposite to Problem I and Problem II. The reason behind it is that the objective of Problem III is to minimize energy imbalances in balancing power market. Last, Problem IV day-ahead planning outcomes are consistent with Problem II results. However, since the last problem considers the wind energy deviations additionally, day-ahead operation plans changes to minimize wind energy mismatches in the day time in an hourly manner. In this sense, Problem IV has a lower imbalance magnitude than the one in Problem II. However, imbalance cost is higher in Problem IV. The reason behind this difference comes from the price multiplier while calculating the imbalance cost. Since the real time objective function of Problem IV is the minimizing the energy mismatches, minimum imbalance cost is not always guaranteed.

Moreover, all problems are solved with a smaller pump unit, as well. It is observed that smaller pump unit increases the operating range of pumping, which provides more flexible operation, for all the problems. Furthermore, Problem IV is analyzed for two different volume limits margin coefficient sets. It is found that setup with wide range coefficients has a smaller imbalance magnitude and cost. Finally, it can be concluded that operation in January is more profitable for PSPP operation in Problem I, Problem II, and Problem IV. On the other hand, total profit for Problem II and Problem IV are larger in August due to the profit of wind plants. Furthermore, in August energy imbalance magnitude are lower for Problem III.

CHAPTER 5

CONCLUSION AND FUTURE WORK

Integration of renewable energy generation to the power grid makes energy storage an inevitable component of the system. The most mature and widely used energy storage type in the world are pumped storage systems. In parallel to increasing pumped storage capacity trends globally, Turkey plans to ramp up this type of storage technology usage in the near future. Gökçekaya pumped storage power plant is one of the investigated potential projects.

Utilization of Gökçekaya PSPP model for short term control strategies is investigated in this dissertation. For this purpose, models for discharging and pumping modes are constructed. Obtained models are discretized for three different head levels. Further, changes in efficiency for the turbine with respect to discharge rate is also considered by using piecewise linear curves. In this way, a more realistic model of the PSPP is obtained. By using this PSPP model and the wind energy data, four different short term optimization problems are introduced. By using the MILP method, problems are formulated in AMPL language. For day-ahead scheduling, profit maximization is the aim. On the other hand, wind energy imbalance minimization is the target for the real time operation. In this manner, three day operation pattern for each problem is demonstrated and analyzed. Moreover, optimization with a period of one month is performed for January and August. It is observed that January is the more profitable due to electricity market price variations. Furthermore, the effect of smaller pump unit is studied. It can be concluded that additional small pump unit enhances pumping operation for all problems. Moreover, the last problem is examined for two different volume limit margin coefficient sets. It is found that using wide coefficient range decreases the imbalances due to wind energy forecast error.

In light of the study conducted in this thesis, contributions can be listed as follows:

- Constructed nonlinear model for Gökçekaya PSPP is discretized and piecewise linearized in order to reduce the computational burden in optimization without compromising the accuracy of the model. Thereby, variations of head and turbine efficiency are taken into account.
- Obtained realistic model is utilized with wind energy in four different short term optimization problems.
- Optimization of each problem is performed for both January 2019 and August 2018. Resulted profits are compared and discussed. It is resulted that operating in January is more profitable.
- Including a small pump unit to the existing system is studied. It is found that presence of small pump unit supports the system for a.
- Distribution of all wind energy imbalances in Turkey regarding its magnitude for a one year period is obtained. This distribution is utilized to find volume limit margin coefficients which are substituted into the last problem. It is concluded that wide range setup is more successful regarding minimization of wind energy imbalance.

Based on the studies in this thesis, the proposed model can be improved and extended further. The number of discrete head level may be increased to obtain more accurate model. Switching cost between pumping and discharging modes can be included to the optimization problem. Another improvement might be modelling the natural inflow and spillage. Last but not least, market price or wind energy generation can be forecasted accurately.

REFERENCES

[1] IEA, "Global Energy & CO2 Status Report," , IEA, 2018. Last Accessed on July 31, 2019. [Online]. Available: http://www.indiaenvironmentportal.org.in/files/file/Global_Energy_and_CO2_Status_Report_2018.pdf.

[2] A. Olhoff, "Emissions Gap Report 2018," , UN environment, 2018. Last Accessed on July 31, 2019. [Online]. Available: https://www.ipcc.ch/site/assets/uploads/2018/12/UNEP-1.pdf.

[3] European Environmental Agency, "Renewable energy in Europe - 2018," , EEA, 2018. Last Accessed on July 31, 2019. [Online]. Available: http://www.eea.europa.eu/publications/renewable-energy-in-europe-2016/download.

[4] S. Vezmar, A. Spajić, D. Topić, D. Šljivac, and L. Jozsa, "Positive and Negative Impacts of Renewable Energy Sources," *International journal of electrical and computer engineering systems*, vol. 5, no. 2, pp. 15–23, 2014.

[5] IEA, "Technology Roadmap," , IEA, 2014. Last Accessed on July 31, 2019. [Online]. Available: https://www.iea.org/publications/freepublications/publication/TechnologyRoadmapEnergystorage.pdf.

[6] EASE, "Energy Storage Technologies." *ease-storage.eu*. Last Accessed on August 12, 2019. [Online]. Available: http://ease-storage.eu/energy-storage/technologies.

[7] DOE, "DOE Global Energy Storage Database." *energystorageexchange.org*. Last Accessed on August 12, 2019. [Online]. Available: https://energystorageexchange.org/projects.

[8] M. Rogner and N. Troja, "The world's water battery: Pumped hydropower storage and the clean energy transition," , IHA, 2018. Last Accessed on July 31, 2019. [Online]. Available: https://www.hydropower.org/sites/default/files/

publications-docs/the_worlds_water_battery_-_pumped_storage_and_the_clean_energy_transition_2.pdf.

[9] E. Sulukan, "An analysis of centennial wind power targets of Turkey," *Turkish Journal of Electrical Engineering and Computer Sciences*, vol. 26, no. 5, pp. 2726–2736, 2018.

[10] M. Gimeno-Gutiérrez and R. Lacal-Arántegui, "Assessment of the European potential for pumped hydropower energy storage," , European Commission Joint Research Centre Institute for Energy and Transport, 2013. Last Accessed on July 31, 2019. [Online]. Available: https://ec.europa.eu/jrc/sites/jrcsh/files/jrc_20130503_assessment_european_phs_potential.pdf.

[11] JICA, "The Study on Optimal Power Generation for Peak Demand in Turkey," , JICA, 2011. Last Accessed on July 31, 2019. [Online]. Available: http://open_jicareport.jica.go.jp/pdf/12019790.pdf.

[12] W. Bogenrieder, "Pumped storage power plants," in *Renewable Energy* (K. Heinloth, ed.), pp. 165–196, Springer Berlin Heidelberg, 2006.

[13] J. Pérez-Díaz, G. Cavazzini, F. Blázquez, C. Platero, J. Fraile-Ardanuy, J. Sánchez, and M. Chazarra, "Technological developments for pumped-hydro energy storage," , Mechanical Storage Subprogramme, Joint Programme on Energy Storage, European Energy Research Alliance, 2014. Last Accessed on July 31, 2019. [Online]. Available: https://www.eera-set.eu/wp-content/uploads/Technological-Developments-for-Pumped-Hydro-Energy-Storage_EERA-report-2014.pdf.

[14] A. Oberhofer and P. Meisen, "Energy Storage Technologies & Their Role in Renewable Integration," , Global Energy Network Institute, 2012. Last Accessed on July 31, 2019. [Online]. Available: https://www.geni.org/globalenergy/research/energy-storage-technologies/Energy-Storage-Technologies.pdf.

[15] IEA, "Technology Roadmap Hydropower," , IEA, 2012. Last Accessed on July 31, 2019. [Online]. Available: https://www.iea.org/publications/freepublications/publication/2012_Hydropower_Roadmap.pdf.

[16] EASE, "Pumped Hydro Storage," , European Associaton for Storage of Energy, 2016. Last Accessed on July 31, 2019. [Online]. Available: http://ease-storage.eu/wp-content/uploads/2016/07/EASE_TD_Mechanical_PHS.pdf.

[17] Yenilenebilir Enerji Genel Müdürlüğü, "Pompaj Depolamalı Hidroelektrik Santralleri (PHES) Yol Haritası Çalıştay Raporu," , Enerji ve Tabii Kaynaklar Bakanlığı, 2018. Last Accessed on July 31, 2019. [Online]. Available: https://www.enerjiportali.com/wp-content/uploads/2018/10/PHES_Yol_Haritasi_Calistay_Raporu.pdf.

[18] G. W. Chang, M. Aganagic, J. G. Waight, J. Medina, T. Burton, S. Reeves, and M. Christoforidis, "Experiences with Mixed Integer Linear Programming Based Approaches on Short-Term Hydro Scheduling," *IEEE Transactions on Power Systems*, vol. 16, no. 4, pp. 743–749, 2001.

[19] A. J. Conejo, J. M. Arroyo, J. Contreras, and F. A. Villamor, "Self-scheduling of a hydro producer in a pool-based electricity market," *IEEE Transactions on Power Systems*, vol. 17, no. 4, pp. 1265–1271, 2002.

[20] A. Borghetti, C. D'Ambrosio, A. Lodi, and S. Martello, "An MILP Approach for Short-Term Hydro Scheduling and Unit Commitment With Head-Dependent Reservoir," *IEEE Transactions on Power Systems*, vol. 23, no. 3, pp. 1115–1124, 2008.

[21] C. H. Chen, N. Chen, and P. B. Luh, "Head Dependence of Pump-Storage-Unit Model Applied to Generation Scheduling," *IEEE Transactions on Power Systems*, vol. 32, no. 4, pp. 2869–2877, 2017.

[22] B. Tong, Q. Zhai, and X. Guan, "An MILP based formulation for short-term hydro generation scheduling with analysis of the linearization effects on solution feasibility," *IEEE Transactions on Power Systems*, vol. 28, no. 4, pp. 3588–3599, 2013.

[23] J. García-González and G. A. Castro, "Short-term hydro scheduling with cascaded and head-dependent reservoirs based on mixed-integer linear programming," in *2001 IEEE Porto Power Tech Proceedings*, 2001.

[24] A. Hamann and G. Hug, "Real-time optimization of a hydropower cascade using a linear modeling approach," in *2014 Power Systems Computation Conference*, 2014.

[25] E. D. Castronuovo and J. A. Lopes, "On the optimization of the daily operation of a wind-hydro power plant," *IEEE Transactions on Power Systems*, vol. 19, no. 3, pp. 1599–1606, 2004.

[26] F. Bourry, L. M. Costa, and G. Kariniotakis, "Risk-based strategies for wind/pumped-hydro coordination under electricity markets," in *2009 IEEE Bucharest Power Tech*, 2009.

[27] Á. J. Duque, E. D. Castronuovo, I. Sánchez, and J. Usaola, "Optimal operation of a pumped-storage hydro plant that compensates the imbalances of a wind power producer," *Electric Power Systems Research*, vol. 81, no. 9, pp. 1767–1777, 2011.

[28] A. K. Varkani, A. Daraeepour, and H. Monsef, "A new self-scheduling strategy for integrated operation of wind and pumped-storage power plants in power markets," *Applied Energy*, vol. 88, no. 12, pp. 5002–5012, 2011.

[29] E. D. Castronuovo, J. Usaola, R. Bessa, M. Matos, I. C. Costa, L. Bremermann, J. Lugaro, and G. Kariniotakis, "An integrated approach for optimal coordination of wind power and hydro pumping storage," *Wind Energy*, vol. 17, no. 6, pp. 829–852, 2014.

[30] EPİAŞ, "2017 Yılı Faaliyet Raporu," , EPİAŞ, 2017. Last Accessed on July 31, 2019. [Online]. Available: https://www.epias.com.tr/wp-content/uploads/2018/03/2017_Yili_Yonetim_Kurulu_Faaliyet_Raporu.pdf.

[31] EPİAŞ, "Processes." *www.epias.com.tr*, 2016. Last Accessed on August 10, 2019. [Online]. Available: https://www.epias.com.tr/en/day-ahead-market/processes.

[32] EPİAŞ, "Gün öncesi elektrik piyasası piyasa takas fiyatı belirleme yöntemi," , EPİAŞ, 2016. Last Accessed on July 31, 2019. [Online]. Available: https://www.epias.com.tr/wp-content/uploads/2016/03/public_document_v4_released.pdf.

[33] E. İlseven, "Intraday Markets and Potential Benefits for Turkey," Master's thesis, Middle East Technical University, 2014.

[34] EPİAŞ, "Orders." *www.epias.com.tr*, 2016. Last Accessed on August 10, 2019. [Online]. Available: https://www.epias.com.tr/en/intra-day-market/orders.

[35] F. Yazitas, "Elektrik Piyasaları," , EPİAŞ, 2018. Last Accessed on July 31, 2019. [Online]. Available: https://www.dunyaenerji.org.tr/wp-content/uploads/2018/02/FatihYazitasSunum.pdf.

[36] EPİAŞ, "Annual Electricity Market Report 2018," , EPİAŞ, 2018. Last Accessed on July 31, 2019. [Online]. Available: https://www.epias.com.tr/wp-content/uploads/2019/06/EPIAS_Annual_Electricity_Marker_Report_2018.pdf.

[37] G. O. Brown, "The history of the Darcy-Weisbach equation for pipe flow resistance," *Proceedings of the Environmental and Water Resources History*, pp. 34–43, 2002.

[38] L. F. Moody, "Friction factors for pipe flow," *Transactions of the A.S.M.E*, pp. 671–684, 1944.

[39] T. Davis, "Moody Diagram." *www.mathworks.com*, 2005. Last Accessed on July 31, 2019. [Online]. Available: https://www.mathworks.com/matlabcentral/fileexchange/7747-moody-diagram.

[40] JICA, *Guideline and Manual for Hydropower Development Vol. 1 Conventional Hydropower and Pumped Storage Hydropower*. JICA.

[41] JICA, "Final Report on Feasibility Study on Adjustable Speed Pumped Storage Generation Technology," , JICA, 2012. Last Accessed on July 31, 2019. [Online]. Available: http://open_jicareport.jica.go.jp/pdf/12044822.pdf.

[42] D. Özkaya, "Hidroelektrik santrallerindeki hız regülatörlerinin yenilenmesine ilişkin modelleme ve saha çalışmaları," Master's thesis, Ankara University, 2016.

[43] U. Ramer, "An iterative procedure for the polygonal approximation of plane curves," *Computer Graphics and Image Processing*, vol. 1, pp. 244–256, 1972.

[44] D. H. Douglas and T. K. Peucker, "Algorithms for the reduction of the number of points required to represent a digitized line or its caricature," *The Canadian Cartographer*, vol. 0, no. 2, pp. 112–122, 1973.

[45] TÜREB, "Türkiye Rüzgar Enerjisi İstatistik Raporu 2019," , TÜREB, 2019. Last Accessed on July 31, 2019. [Online]. Available: http://www.tureb.com.tr/files/bilgi_bankasi/turkiye_res_durumu/istatistik_raporu_ocak_2019.pdf.

[46] R. Fourer, D. M. Gay, and B. W. Kernighan, *AMPL A Modeling Language for Mathematical Programming*. 2003.

[47] IBM, *IBM ILOG CPLEX Optimization Studio CPLEX User's Manual*. IBM.

[48] J. Czyzyk, M. P. Mesnier, and J. J. More, "The NEOS server," *IEEE COMPUTATIONAL SCIENCE & ENGINEERING*, vol. 5, no. 3, pp. 68–75, 1998.

[49] E. D. Dolan, "NEOS Server 4.0 administrative guide," , Mathematics and Computer Science Division, Argonne National Laboratory, 2002. Last Accessed on July 31, 2019. [Online]. Available: http://arxiv.org/abs/cs/0107034.

[50] W. Gropp and J. J. Moré, "Optimization Environments and the NEOS Server," in *Approximation Theory and Optimization* (M. D. Buhman and A. Iserles, eds.), pp. 167–182, Cambridge University Press, 1997.

[51] H. Schlunegger, "Pumping efficiency: A 100 MW converter for the Grimsel 2 pumped storage plant," pp. 42–47, 01 2014.

[52] Enerji Atlası, "Rüzgar Enerji Santralleri." *www.enerjiatlasi.com*. Last Accessed on July 31, 2019. [Online]. Available: https://www.enerjiatlasi.com/ruzgar.

APPENDIX A

MOODY DIAGRAM

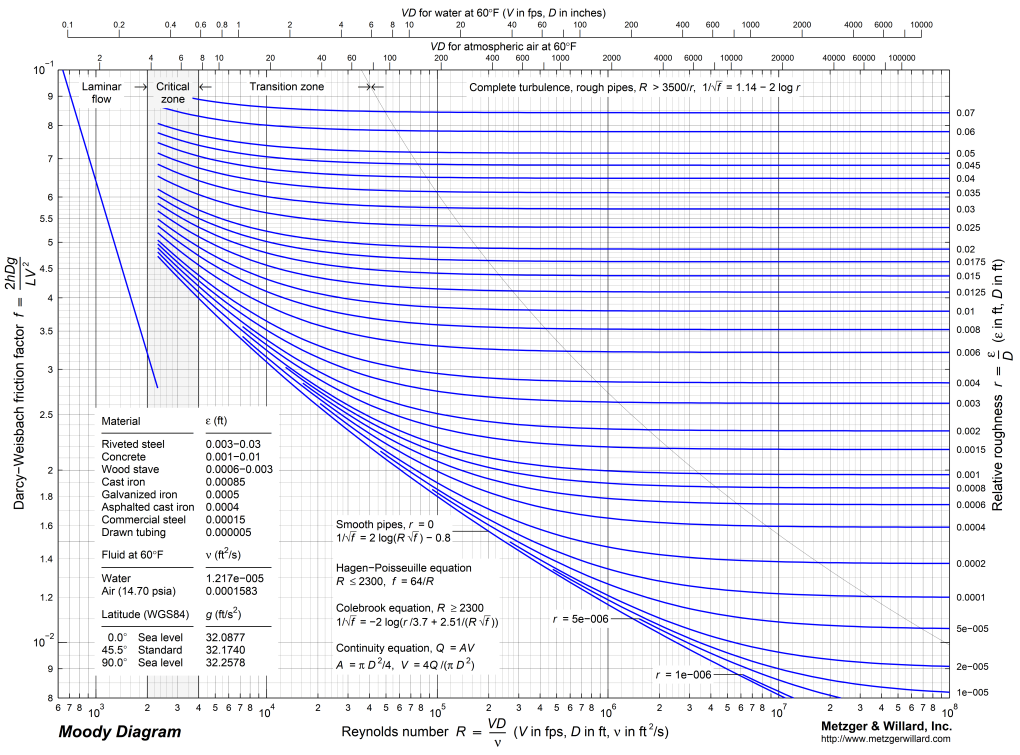

Figure A.1: Moody Diagram [39]

APPENDIX B

TECHNICAL DATA FOR GÖKÇEKAYA PSPP

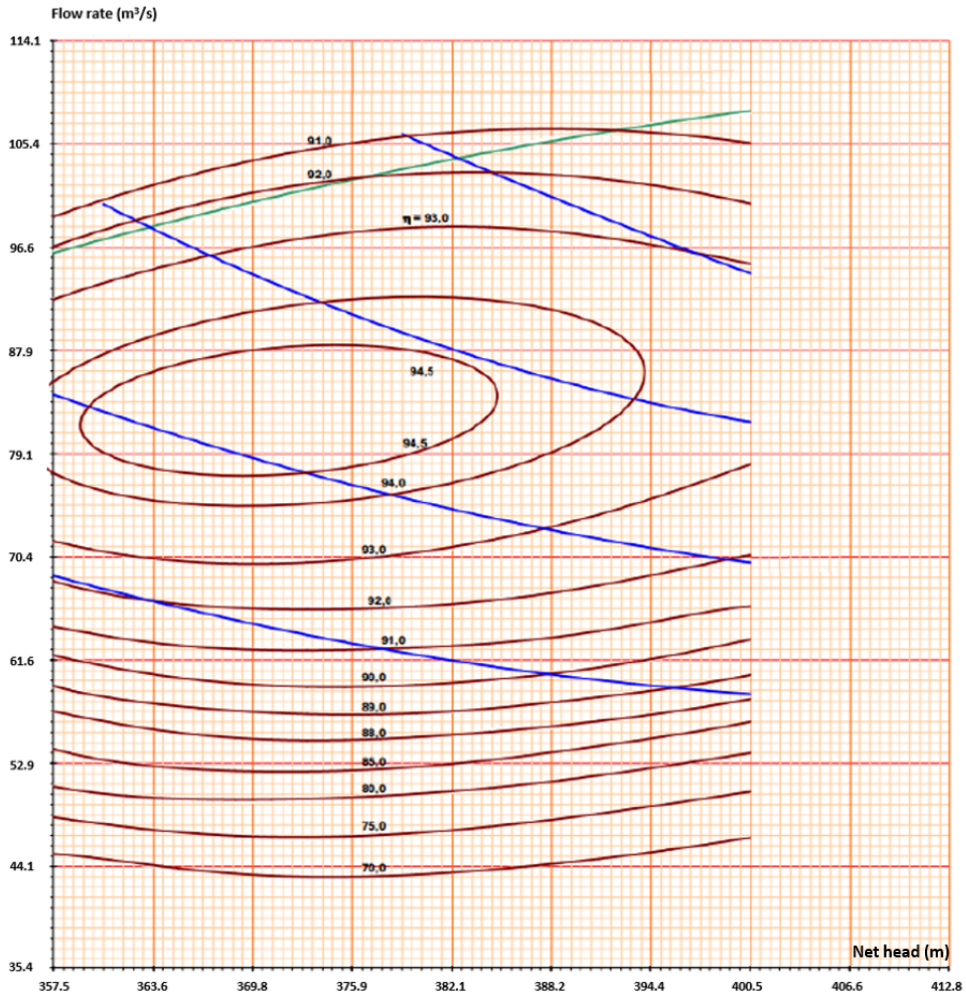

Figure B.1: Turbine Hill Chart Modified to Gökçekaya PSPP [42]

.

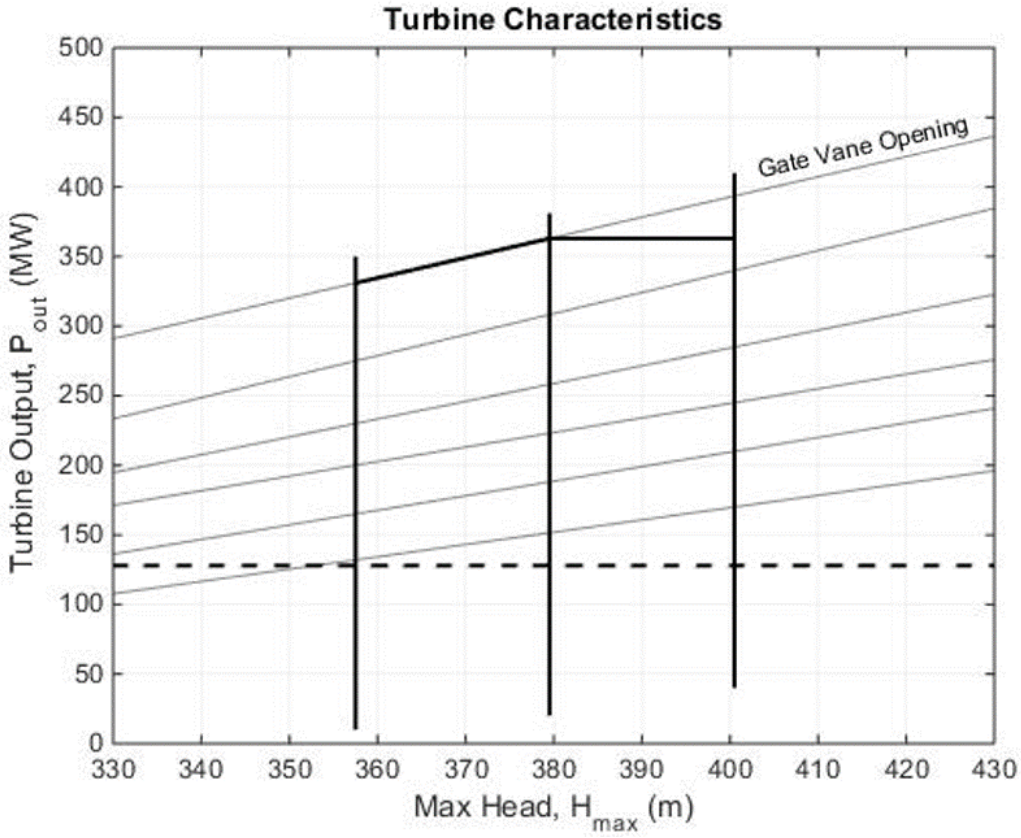

Figure B.2: Turbine Design for Gökçekaya PSPP [41]

.

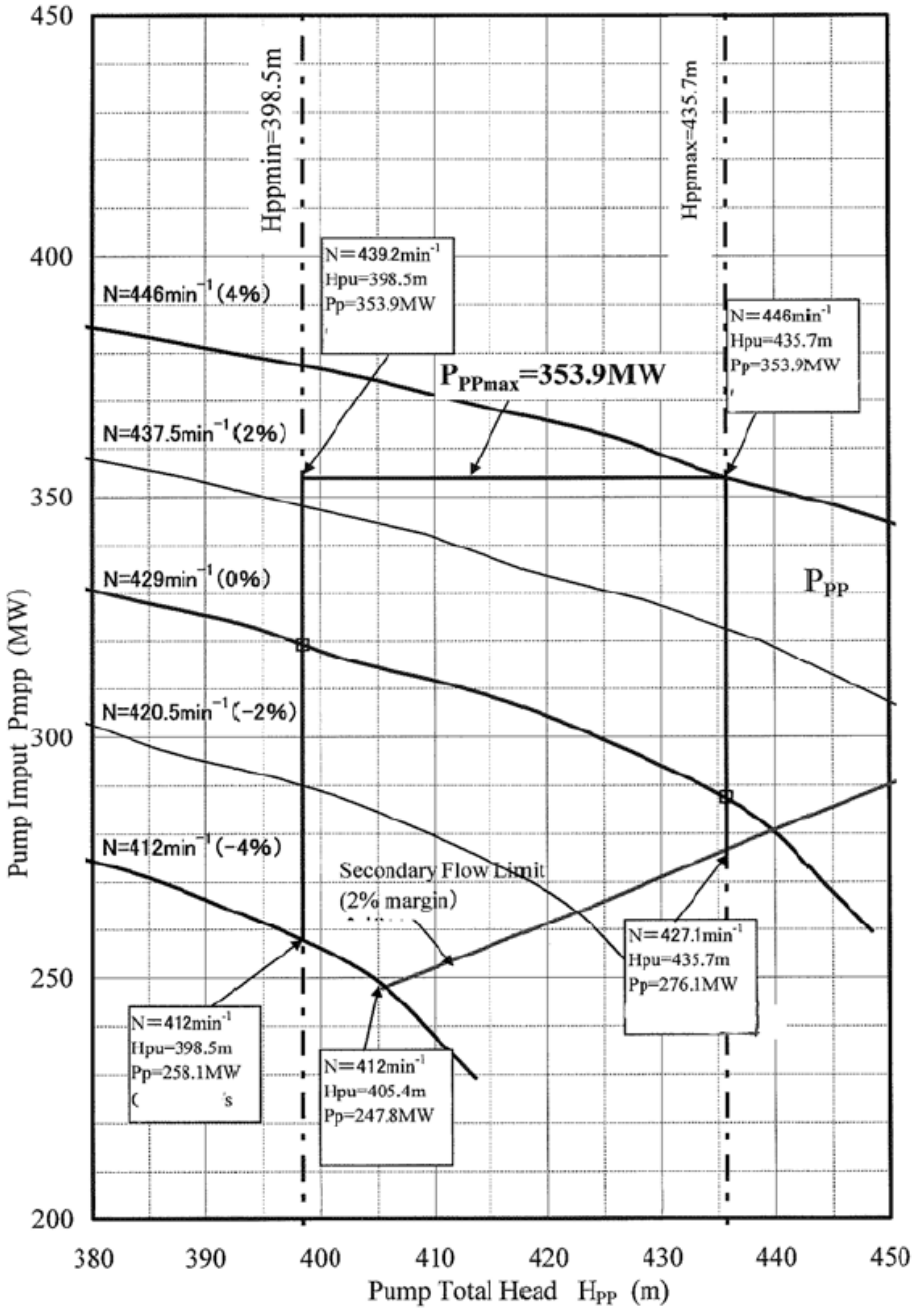

Figure B.3: Pump Design for Gökçekaya PSPP [11]

.

APPENDIX C

WIND POWER PLANT DATA

Table C.1: Wind Power Plant Under Operation in Turkey [45].

Polat Enerji			
Company Name	**Project Name**	**City**	**Installed Capacity (MW)**
Soma En. El. Ür. A.Ş.	Soma RES	Manisa	264.1
Al-Yel El. Ür. A.Ş.	Geycek RES	Kırşehir	168
Poyraz En. El. Ür. A.S.	Poyraz RES	Balıkesir	38.55
Doğal En. El. Ür. A.Ş.	Sayalar RES	Manisa	28.6
Doğal En. El. Ür. A.Ş.	Samurlu RES	İzmir	21.95
Doruk En. Ür. San. Tic. A.Ş.	Seyitali RES	İzmir	20.75
Doğal En. El. Ür. A.Ş.	Kozbeyli RES	İzmir	17.28
Doğal En. El. Ür. A.Ş.	Burgaz RES	Çanakkale	7.45
Demirer Enerji			
Company Name	**Project Name**	**City**	**Installed Capacity (MW)**
Mare Manastır Rüz. En. San. Tic. A.Ş.	Mare Manastır RES	İzmir	56.2
Alize En. El. Ür. A.Ş	Kuyucak RES	Manisa	50.3
Alize En. El. Ür. A.Ş..	Çamseki RES	Çanakkale	42.3

Dares Datça Rüz. En. Sant. San. ve Tic. A.Ş.	Dares Datça RES	Çanakkale	41.6
Poyraz En. El. Ür. A.S.	Poyraz RES	Muğla	38.55
Alize En. El. Ür. A.Ş.	Sarıkaya RES	Balıkesir	30
Alize En. El. Ür. A.Ş.	Keltepe RES	Tekirdağ	29.9
Doğal En. El. Ür. A.Ş.	Sayalar RES	Balıkesir	28.6
Anemon En. El. Ür. A.Ş.	İntepe RES	Manisa	27.85
Ufuk En. El. Ür. A.Ş.	Poyrazgölü RES	Çanakkale	24.25
Doğal En. El. Ür. A.Ş.	Samurlu RES	Balıkesir	21.95
Alize En. El. Ür. A.Ş.	Çamseki RES	Çanakkale	20.8
Doruk En. Ür. San. Tic. A.Ş.	Seyitali RES	Çanakkale	20.75
Doğal En. El. Ür. A.Ş.	Kozbeyli RES	İzmir	17.27
Alize En. El. Ür. A.Ş.	Çataltepe RES	İzmir	16
Alize En. El. Ür. A.Ş.	Çeşme RES	Balıkesir	10.7
Bores Bozcaada Rüz. En. San.Tic. A.Ş.	Bozcaada RES	İzmir	10.2
Doğal En. El. Ür. A.Ş.	Burgaz RES	Çanakkale	7.45
Güriş			
Company Name	**Project Name**	**City**	**Installed Capacity (MW)**
Olgu En. Ür. Tic. A.Ş.	Dinar RES	Afyon	200.25
Derne En. Ür. Tic. A.Ş.	Fatma RES	Muğla	80
Derne En. Ür. Tic. A.Ş.	Kanije RES	Edirne	64
Belen El. Ür. A.Ş.	Belen RES	Hatay	48
Eolos Rüz. En. Ür. A.Ş.	Senkoy RES	Hatay	36
Derne En. Ür. Tic. A.Ş.	Zeliha RES	Kırklareli	25.6
Güriş İnş. Müh. A.Ş	Atik RES	Hatay	18
Ayres Ayvacık El. Ür. Sant. Ltd. Şti.	AyRES	Çanakkale	5.4
Ayvacık Elektrik Üretim A.Ş.	Seyit Onbaşı RES	Çanakkale	4

Borusan EnBW Enerji			
Company Name	**Project Name**	**City**	**Installed Capacity (MW)**
Borasco En. Ve Kim. San. Tic. A.Ş.	Bandırma RES	Balıkesir	89.7
Efil Enerji Üretim Ticaret ve Sanayi A.Ş.	Kartaldagi RES	Gaziantep	65.55
Borusan EnBW	Balabanlı RES	Tekirdağ	61.4
Eskoda Enerji Ür. Paz. İth. İhr. A.Ş.	Harmanlık RES	Bursa	52.8
Eskoda Enerji Ür. Paz. İth. İhr. A.Ş.	Koru RES	Çanakkale	52.8
Güney Rüzgarı El. Ür. Tic. Aş.	Mut RES	Mersin	52.8
FuatRES Elektrik Üretim A.Ş.	Fuat RES	İzmir	33
Alenka Enerji Ür. ve Yat. Ltd. Şti.	Kıyıköy RES	Kırklareli	28

Table C.2: Wind Power Plant Under Construction in Turkey [45].

Borusan EnBW Enerji			
Company Name	**Project Name**	**City**	**Capacity (MW)**
Borusan EnBW	Balabanlı RES-faz3	Tekirdağ	25.2
Eksim Holding			
Company Name	**Project Name**	**City**	**Capacity (MW)**
Çeşme Enerji A.Ş.	Ovacık RES	Kahramanmaraş	28.8

Table C.3: Licensed Wind Power Plant in Turkey [45].

Güriş			
Company Name	**Project Name**	**City**	**Capacity (MW)**
Yuva Enerji Yatırım Üretim ve Tic. A.Ş.	Yuvacık RES	Kocaeli	120
İzdem Enerji Yatırım Üretim ve Tic. A.Ş.	Kocatepe RES	Afyonkarahisar	109
Borusan EnBW Enerji			
Company Name	**Project Name**	**City**	**Capacity (MW)**
Boylam Enerji Yatırım Üretim Tic. A.Ş.	Saros RES	Çanakkale	138

Table C.4: Prelicensed Wind Power Plant in Turkey [45].

Investor Name	**Capacity (MW)**
Polat Enerji	572.9
Demirer Enerji	80
Borusan EnBW Enerji	393.46

Table C.5: Selected Under Operation Wind Power Plants to Simulate Under Constrction, Licensed, and Prelicensed Capacity [52]

Fina Enerji			
Company Name	**Project Name**	**City**	**Installed Capacity (MW)**
Ziyaret RES El. Ür. San. ve Tic. A.Ş.	Ziyaret (Türbe) RES	Hatay	76

Kavram En. Yat. Ür. ve Tic. A.Ş.	Uluborlu RES	Isparta	60
Ütopya El. Ür. San. ve Tic. A.Ş.	Düzova RES	İzmir	51.5
Çanres Rüzgar En. Ür. San. ve Tic. A.Ş.	Şadıllı RES	Edirne	33
Borares En. El. Ür. A.Ş.	Karova RES	Muğla	30
Manres El. Ür. A.Ş.	Günaydın RES	Balıkesir	20
ÖRES El. Ür. A.Ş.	Salman RES	İzmir	20
Aysu En. San. ve Tic. A.Ş.	Karadere RES	Kırklareli	19.2
Serin En. El. Ür. A.Ş.	Ortamandıra RES	Balıkesir	10
Dost Enerji			
Company Name	**Project Name**	**City**	**Installed Capacity (MW)**
Bergres El. Ür. A.Ş.	Bergres RES	İzmir	69.95
İnnores El. Ür. A.Ş.	Yuntdağ RES	İzmir	60
Geres El. Ür. A.Ş.	Geres RES	Manisa	30
Kores Kocadağ RES Üretim A.Ş.	Kores Kocadağ RES	İzmir	25
Alto Holding			
Company Name	**Project Name**	**City**	**Installed Capacity (MW)**
Lodos Karaburun El. Ür. A.Ş.	Karaburun RES	İzmir	120
Lodos El. Ür. A.Ş.	Kemerburgaz RES	İstanbul	24
Doğan Holding			
Company Name	**Project Name**	**City**	**Installed Capacity (MW)**

Galata Wind Enerji A.Ş.	Şah RES	Balıkesir	93
Galata Wind Enerji A.Ş.	Mersin RES	Mersin	34
FC Enerji			
Company Name	**Project Name**	**City**	**Installed Capacity (MW)**
Bak Enerji Üretimi A.Ş.	Kayseri Yahyalı RES	Kayseri	82.5
Sabaş Elektrik Üretim A.Ş.	Turguttepe RES	Aydın	24
YGT Elektrik Üretim A.Ş.	Adares RES	İzmir	10
Sancak Enerji			
Company Name	**Project Name**	**City**	**Installed Capacity (MW)**
SE Santral El. Ür. San. ve Tic. A. Ş.	Sancak Enerji Yahyalı RES	Kayseri	52.5
ES-YEL El. Ür. A.Ş.	Ardıçlı RES	Konya	43.91
Hassas Teknik En. El. Ür. San. ve Tic. A.Ş.	Urla RES	İzmir	15
Erdem Holding			
Company Name	**Project Name**	**City**	**Installed Capacity (MW)**
Kütle Enerji Yatırım Üretim ve Ticaret A.Ş.	Bağarası RES	Aydın	46
Tayf En. Yat. Ür. ve Tic. A.Ş.	Ödemiş RES	İzmir	42
Eber El. Ür. A.Ş.	Eber RES	Afyonkarahisar	36
Edincik Enerji			

Company Name	Project Name	City	Installed Capacity (MW)
Edincik En. Ür. A.Ş.	Edincik RES	Balıkesir	77.4